Limited impact on oysters in first-of-its-kind field trial of marine carbon dioxide removal (mCDR) strategy

Authors: Emilia Jankowska[1*], Matthew Sclafani[2], Bonnie X. Chang[1], Hailey Hayes[1], Robert Cerrato[3], Nicholas S. Fisher[3], Chloe Leach[1], Devon B. Cole[1], Brian P. Jackson[4], Christopher Gobler[3], Adam V. Subhas[5], Matthew G. Hayden[5], M. Grace Andrews[1]

Affiliations:

[1]Hourglass Climate, NPO, Montclair, NJ, USA
[2]Cornell Cooperative Extension, Riverhead, NY, USA
[3]School of Marine and Atmospheric Sciences, Stony Brook University, Stony Brook, NY, USA
[4]Dartmouth College, Hannover, NH, USA
[5]Department of Marine Chemistry and Geochemistry, Woods Hole Oceanographic Institution, Woods Hole, MA, USA

*Corresponding author: emilia@hourglassclimate.org

Abstract

Carbon dioxide removal (CDR) is a necessary component of limiting global warming to 2°C by 2100. Marine enhanced rock weathering (mERW) with minerals like olivine is a CDR strategy with the potential to capture atmospheric carbon dioxide and mitigate ocean acidification, which threatens calcifying organisms including those essential for global aquaculture such as oysters. mERW could benefit these species, although olivine releases trace metals like nickel which may bioaccumulate. This study reports findings from the world's first field trial of mERW, conducted in NY, USA. After a year of exposure to olivine, Eastern oysters showed no significant difference in biomass between Olivine and Control treatments, and mean metal accumulations were below US Food and Drug Administration warning thresholds and within global natural ranges. Our findings suggest that mERW with olivine has a limited effect on oysters and olivine-derived metals did not result in oyster safety concerns for human health.

Keywords: Carbon dioxide removal, marine enhanced rock weathering, ocean alkalinity enhancement, olivine, trace metals, bioaccumulation, shellfish, Eastern oyster

Introduction

Limiting Earth's temperature increase to 2°C by 2100 requires drastic greenhouse gas emission reductions and the removal of approximately 10 Gt CO_2 per year by mid-century and 20 Gt CO_2 per year by the end of the century[1]. Therefore, implementing effective, safe and scalable carbon dioxide removal (CDR) strategies is imperative. One CDR strategy is ocean alkalinity enhancement (OAE), which involves increasing the concentration of seawater alkalinity and ultimately driving an influx of carbon dioxide (CO_2) from the atmosphere into the ocean[2]. Marine enhanced rock weathering (mERW) is a specific form of OAE where alkaline rocks and/or minerals are introduced into the ocean to dissolve and generate alkalinity[3–6]. Recent research indicates that mERW has the potential to sequester between 0.3 to 10 Gt of CO_2 y^{-1} from the atmosphere[7,8]. One mineral commonly proposed for mERW is olivine, a naturally occurring ultramafic silicate ($Mg_{2-x}Fe_xSiO_4$). Olivine dissolves in seawater over months to years, releasing cations (such as magnesium (Mg^{2+}) and iron (Fe^{2+})) and generating alkalinity (mainly bicarbonate (HCO_3^-))[5,9]. As companies worldwide form to commercialize and ultimately scale mERW through an actively growing carbon market, there is an urgency to understand the potential impacts this approach has on the marine environment.

Through the introduction of alkalinity, OAE strategies such as mERW may offer the critical co-benefit of localized ocean acidification mitigation due to the resulting increase in carbonate and bicarbonate ions. Ocean acidification negatively affects calcifying organisms such as bivalves[10,11] by reducing their calcification and growth rates[12]. Adult bivalves have a range of physiological mechanisms to cope with ocean acidification, however, these processes can be energetically expensive and necessitate energy reallocation[11,13]. Oysters, in particular, are vulnerable to acidification impacts, a critical concern for the shellfish industry due to the predicted production declines of 14-28% by 2100 in certain regions if acidification trends continue[14–16]. This decrease poses a risk to both the global economy and food security, as the aquaculture sector—which employed over 20 million people and generated USD 281.5 billion in 2020[17]—relies heavily on shellfish. In North America and beyond, oysters represent a significant portion of aquaculture production, with an estimated 18 million tonnes of marine mollusks produced worldwide in 2020[17]. As such, there is increasing interest in strategies to enhance alkalinity in oyster aquaculture environments[18] and mERW could locally raise alkalinity levels to create more favorable conditions for oyster growth. Regional alkalinity enhancement holds promise in supporting shellfish resilience, potentially alleviating some of the most damaging effects of acidification on this ecologically and economically essential industry.

Beyond ocean alkalinity enhancement, mERW with minerals such as olivine could exert ecological impacts through the release of elements found in olivine, namely silicon (Si) and trace metals, particularly nickel (Ni), chromium (Cr), and cobalt (Co). These elements may serve as a source of nutrients for marine organisms, for example, Si could support the growth of silicifying algae and sponges[19]. On the contrary, high concentrations of trace metals may have adverse effects, including bioaccumulation in higher trophic levels and disruptions to ecosystem dynamics[9,20,21]. Organisms have mechanisms for trace metal detoxification, but this process can increase energy expenditure and subsequently impact growth and reproduction[22,23]. To date, the impact of olivine dissolution on marine organisms has mostly been studied in laboratory settings where organisms were kept in closed tanks and often exposed to higher concentrations of olivine dissolution products than what could be expected under natural conditions[24,25] and only one study exposed mussels to olivine in harbor conditions[26]. Field trials, which quantify the environmental impact of mERW under real-world conditions, are the critical next step in assessing the safety, and thereby the true potential, of mERW as a climate mitigation strategy[1].

This study investigates the impact of mERW with olivine sand on oyster growth and trace metal bioaccumulation under natural conditions. Due to their sensitivity to alkalinity levels, their sessile and filter-feeding nature, and their ability to accumulate both essential and non-essential metals, oysters are well suited for studying the impact of mERW with olivine[27,28]. In July 2022, the world's first field trial of mERW was launched. Approximately 650 tonnes of olivine sand was placed along ~300 m of an intertidal beach in the Peconic Bay, Long Island, NY, USA (Fig. 1). Shortly thereafter, Eastern oysters (*Crassostrea virginica* Gmelin, 1791) were transplanted to the Olivine treatment site, as well as three control sites (Control West, Control East 1, and Control East 2) adjacent to the Olivine treatment site. The oysters were subsampled at three-time points over one year and analyzed for growth and soft tissue metal accumulation. In addition, a suite of sediment and sediment porewater parameters were measured to track olivine transport and dissolution through time. This is the first investigation of the impact of mERW on marine biota under real-world conditions.

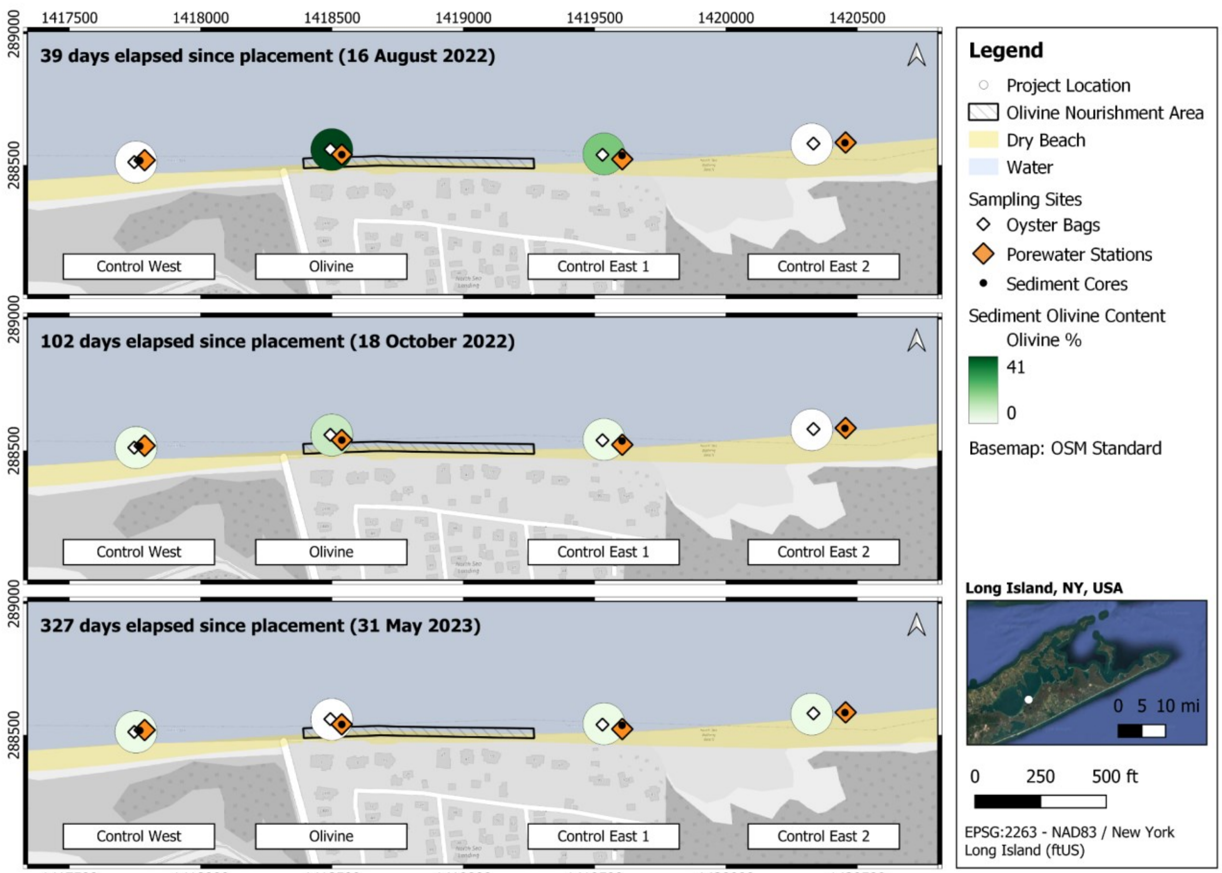

Fig. 1 Study area in the Peconic Bay, Long Island, NY, USA. Bubbles represent the olivine percentage measured by X-Ray Diffraction in the 1-3 cm sediment interval at four treatment sites and three dates throughout the oyster experiment.

Results

Oyster growth

For all sites, oysters grew significantly through time. All sites had higher average oyster dry weights at day 147 and day 300 than day 64 ($p<0.001$, Table 1, Fig. 2). Notably, the difference in dry weight was marginally nonsignificant ($p=0.051$, Table 1) for Olivine treatment oysters compared to Control treatment oysters at 2 months post-placement (day 64). Oysters exposed to the Olivine treatment had dry weights of 1.7 ± 0.5 g compared to those in Control treatments (average dry weight across all Controls: 1.1 ± 0.3 g dw, Fig. 2). No statistical differences between treatments were observed at later time points.

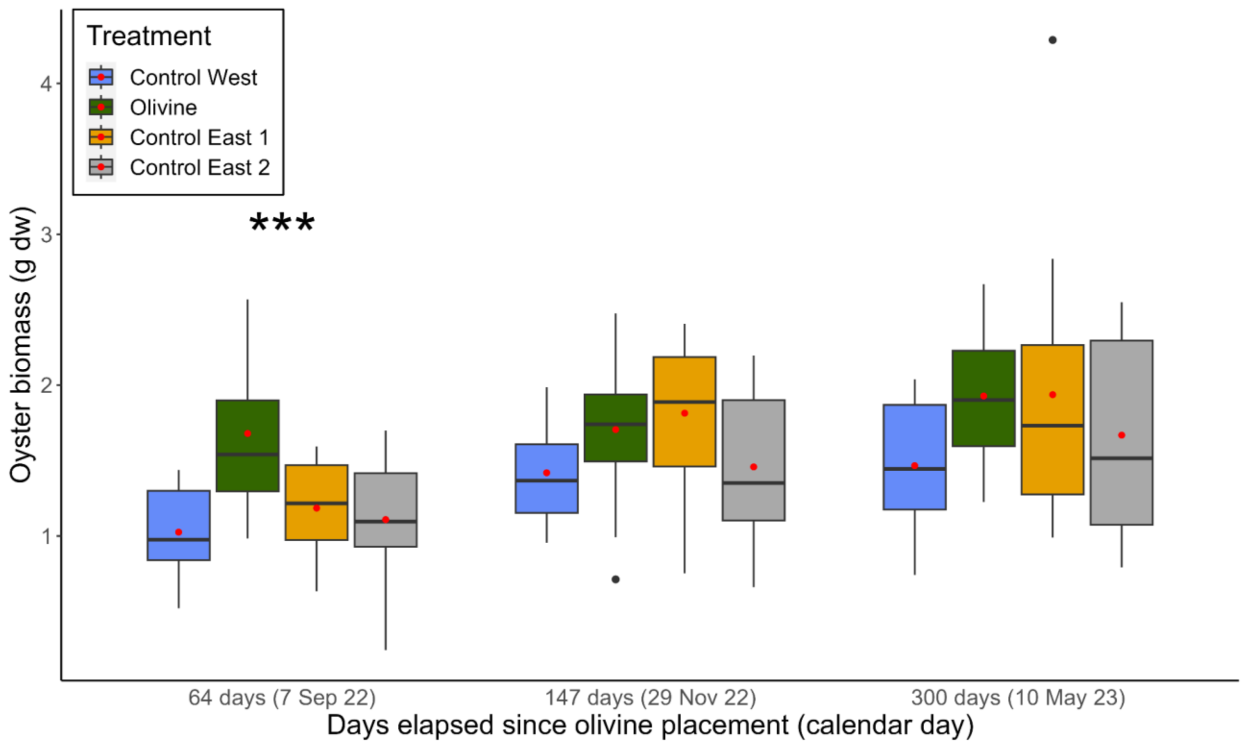

Fig. 2 Oyster dry weight (g dw) measured at each sampling event. Mean (red dot), median (horizontal line), 25th and 75th percentile (box), minimum and maximum value (vertical line), and outliers (black dot) are presented. The asterisk *** indicates significant general linear mixed model (GLMM) results for the Date factor at $p<0.001$. The Treatment factor was marginally nonsignificant at $p=0.051$ on September 7, 2022. Note that the percent of olivine in the sediment at all treatment sites changed throughout the experiment (Fig. 1). The olivine content of the sediment was most enriched at the Olivine treatment site, compared to controls, in the initial weeks of the experiment.

Table 1 Results of the GLMM for oyster biomass and select trace metal body burden tested among four treatments and three dates. Pr values provided, with significant tests marked with bold font and asterisk * showing significance at p<0.05, ** significance at p<0.01, and *** significance at p<0.001. Only significant results for pair-wise tests are provided. For pair-wise results: September stands for September 7th, 2022; November for November 29th, 2022; May for May 10th, 2023.

		Oyster biomass		Ni body burden		Cr body burden		Co body burden	
	df	Chisq	Pr (>Chisq)	Chisq	Pr (>Chisq)	Chisq	Pr (>Chisq)	Chisq	Pr (>Chisq)
Treatment	3	7.765	0.051	0.608	0.895	6.769	0.081	3.645	0.302
Date	2	20.547	**3.452e-05*** **	7.407	**0.025***	10.656	**0.005****	13.257	**0.001****
Treatment X Date	6	7.940	0.242	20.753	**0.002****	18.829	**0.004****	17.245	**0.008****
Pair-wise		For factor Date: September ≠ November, May		For factor Date: September ≠ November, May For factor Treatment:Date: Control West September ≠ Olivine all dates, Control East 1 all dates, Control East 2 all dates		For factor Date: September ≠ November, May For factor Treatment:Date: Control East 1 November ≠ Olivine November; Control East 2 November ≠ Control West September; Control West September ≠ Control West November; Control West September ≠ Olivine November		For factor Date: September ≠ November, May For factor Treatment:Date: Control East 1 September ≠ Olivine May; Control West September ≠ Control East 2 all dates, Control East 1 all dates, Olivine November, May	

Oyster tissue metal bioaccumulation

Approximately 2 months (64 days) after olivine placement the average Ni concentration in oysters at the Olivine treatment site was 3.35 ± 1.89 μg g dw^{-1}. Although this concentration was higher than that observed in Control East 1 and 2 oysters (2.37 ± 0.71 and 2.62 ± 2.79 μg g dw^{-1}, respectively), the differences were not significant ($p>0.05$, Table 1). However, the Ni concentration in Olivine treatment oysters (as well as Control East 1 & 2) was significantly lower than Control West oysters (5.23 ± 2.06 μg g dw^{-1}, Fig. 3A, $p<0.05$, Table 1). The average Ni body burden of Control West oysters declined over time. Approximately 5 months (147 days) after placement, the average Ni body burden of Control West oysters (1.64 ± 0.60 μg g dw^{-1}) was indistinguishable from Olivine and Control East treatment oysters (1.64 ± 1.77 μg g dw^{-1}) ($p>0.05$, Table 1). Ni concentrations remained low in all treatments ~10 months (300 days) after placement, with treatment averages between 2.18 ± 2.71 μg g dw^{-1}. The body burden of other metals associated with olivine (i.e., Co, Cr) presented a pattern similar to Ni (Table 1) and were low (< 1 μg g dw^{-1}) throughout the experiment (Fig. 3B, C). We find that the accumulation of Ni, Cr, and Co directly resulted from olivine because other sources of contamination, such as septic tank discharge or groundwater, would likely have resulted in increased accumulation of non-olivine metals (e.g., aluminum (Al), cadmium (Cd), copper (Cu), lead (Pb), zinc (Zn)), but this was not observed (Fig. S2.1 - S2.6).

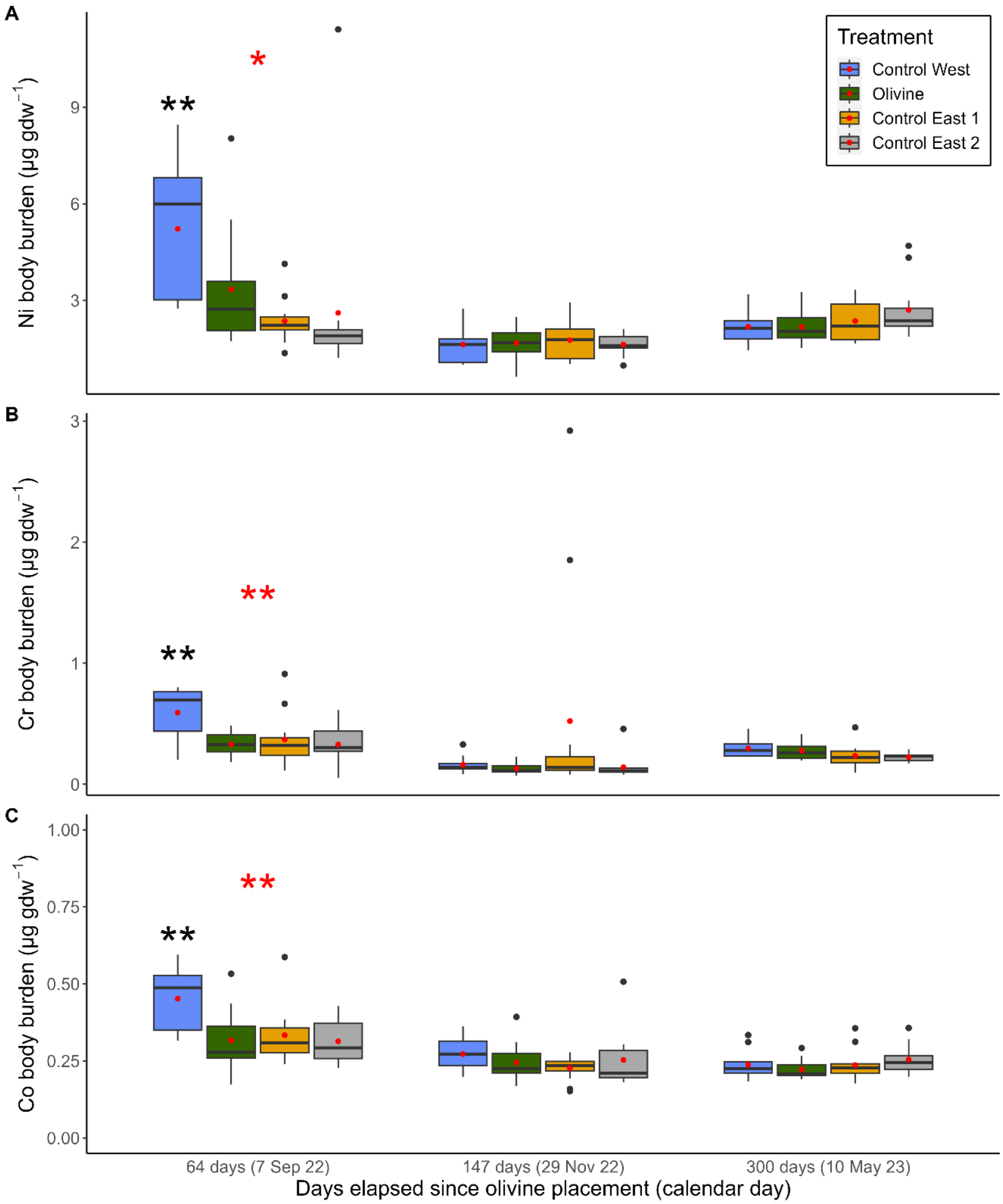

Fig. 3 Oyster tissue trace metal body burden (μg g dw^{-1}) during the experiment: A) Ni, B) Cr, and C) Co. Mean (red dot), median (horizontal line), 25th and 75th percentile (box), minimum and maximum value (vertical line), and outliers (black dot) are presented. 'Sep' stands for September, 'Nov' for November. The top, red asterisk indicates significant GLMM model results for the Date factor, while the bottom, black asterisk is for interaction Date:Treatment. * showing significance at $p<0.05$, ** showing significance at $p<0.01$.

Olivine distribution and its effect on sediment porewater composition

Sediment transport plays an essential role in understanding the exposure of oysters and other marine life to olivine sand following placement in the coastal environment. Hydrodynamics can redistribute the olivine through time, and in turn, the resultant olivine dissolution products (e.g., alkalinity and trace metals). Temporal and spatial changes in sediment olivine content and porewater metal concentrations are essential for contextualizing spatiotemporal trends in oyster growth and trace metal body burden.

Approximately 1 month (39 days/August) after placement, the Olivine treatment site was comprised of 40.5% olivine sand, a substantial amount of olivine had moved to Control East 1 (20.6%), while Control West and Control East 2 had no olivine (0%) (Fig. 1). By ~3 months post-placement (102 days), the concentration of olivine in sediment was still highest at the Olivine treatment site (13.5%) but had decreased substantially since August. Furthermore, the olivine sand had dispersed along more of the coastline, comprising 5.7% of sediment at Control West and 5.1% of sediment at Control East 1. By ~11 months post-placement (327 days) all sites had < 10% olivine in the sediment, with the highest percentage of olivine at Control East 1 (7.1%) and the lowest percentage of olivine sand at the Olivine treatment site (0%). Overall, hydrodynamics increased the overall coastal area with a component of olivine in the sediment through time, while decreasing the amount of olivine at the original placement site. We note that these results represent only the 1-3 cm sediment layer, thus olivine may have been present in deeper sediment layers.

As olivine dissolves in the sediment, the concentration of dissolved species such as total alkalinity (TA), Ni, Cr, and Co in sediment porewater varies substantially over short timescales (minutes to days) due to changes in the concentration of olivine in the sediment, the olivine dissolution rate, natural biogeochemical cycling in the sediment, and physical processes such as advection and bioirrigation which dilute porewater with bottom water. Due to these complex controls, porewater composition mainly serves to establish the presence or absence of olivine dissolution products, and as a qualitative tracer for the relative magnitude of dissolution products between sites.

We observed that the highest concentrations of TA and olivine-derived trace metals (Ni, Cr, Co) were measured in the Olivine treatment porewaters within the first few months of the field trial (Fig. 4, Fig. S1.1), consistent with the high concentration of olivine in the sediment at that point (Fig. 1). More specifically, the highest TA concentrations observed during the experiment were in Olivine treatment porewater on days 14 and 77 of the experiment; they were ~30% - 37% higher than bottom water or Control East 1 and 2 porewater TA concentrations (Fig. 4A). Control

West TA porewater concentrations were also higher than those at Control East 1 and 2 by ~7% on day 14 and ~20% - 27% on day 77 of the experiment. The highest porewater Ni concentration (98.8 $\mu g\ L^{-1}$) was observed at the Olivine treatment site ~1 month (28 days) after olivine placement while Ni concentrations were low at all Control sites (0.4 to 1.4 $\mu g\ L^{-1}$, Fig. 4B). By day 65 post olivine placement, the porewater Ni concentration at the Olivine treatment site had declined to 3.4 $\mu g\ L^{-1}$. From that time point forward, the porewater Ni concentrations remained low at all treatment sites. Similar trends were observed for the other olivine-derived metals, with higher concentrations of Cr and Co in Olivine treatment porewaters than at Control sites during the first month following olivine placement (Fig. S1.1 A, B).

Overall, significantly elevated TA and trace metal (Ni, Cr, Co) concentrations were only observed in porewater, and not in bottom water (0 cm depth), suggesting significant dilution of olivine dissolution products by the water column. Notably, bottom water Ni and Cr concentrations never exceeded the US Environmental Protection Agency (US EPA) National Recommended Water Quality Criteria acute or chronic concentrations for seawater (74 and 8.2 $\mu g\ L^{-1}$ for Ni, 1100 and 50 $\mu g\ L^{-1}$ for Cr (VI), respectively. There are no US EPA Recommended Water Quality Criteria for Co in seawater, however, Saili et al. 2021[29] established a chronic Co surface water concentration of 7 $\mu g\ L^{-1}$. All bottom water Co concentrations were far below this threshold as well. No water quality recommendations exist for porewaters.

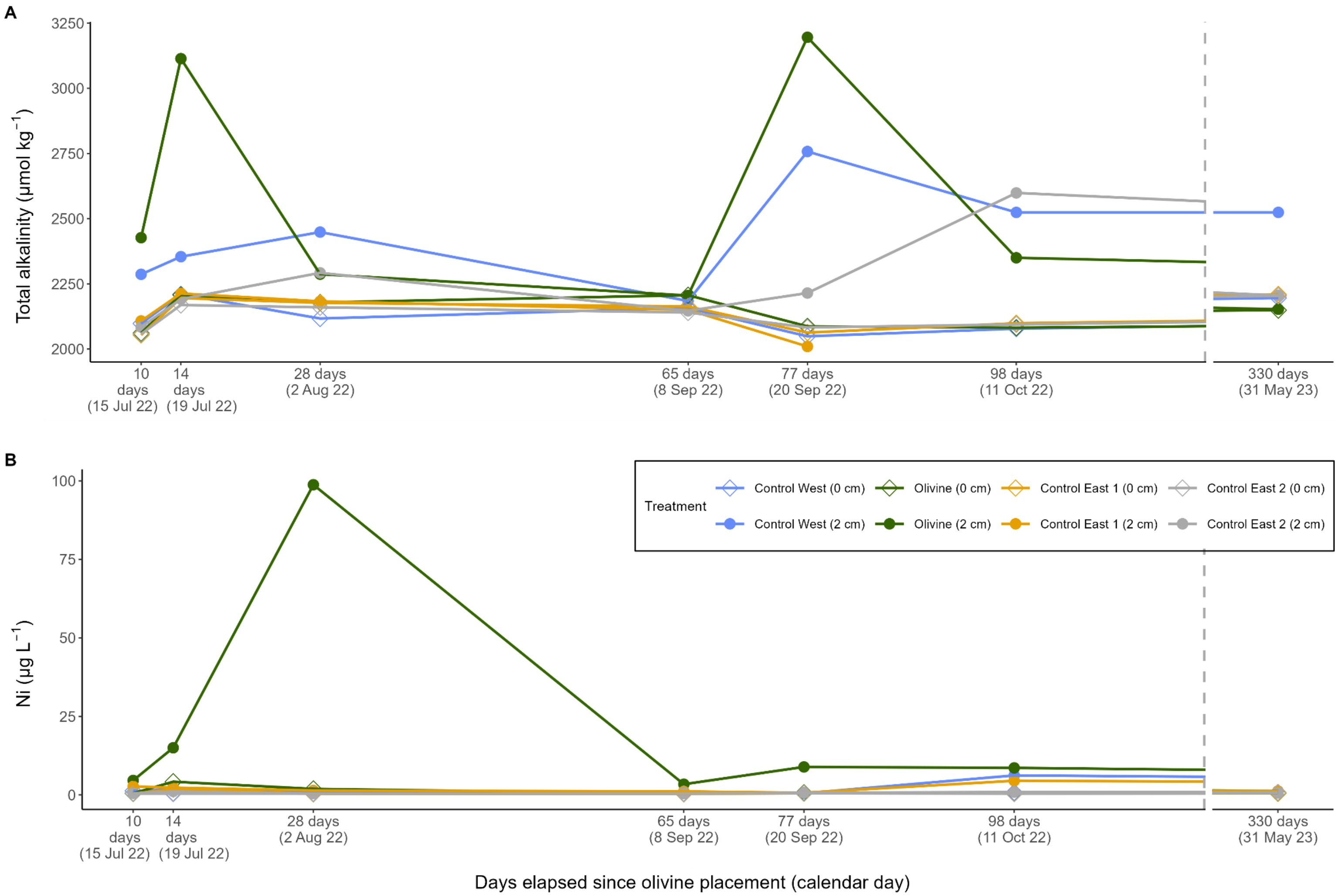

Fig. 4 Olivine dissolution parameters measured during the experiment in bottom water (0 cm) and porewater (2 cm) A) TA (μmol kg^{-1}) and B) Ni concentration (µg L^{-1}). Colors represent four treatments, shapes represent bottom vs. porewater samples. ‘Jul’ stands for July, ‘Aug’ for August, ‘Sep’ for September, ‘Oct’ for October, ‘Nov’ for November. Analytical error bars (SD) for TA are ± 4.4 μmol kg^{-1} (2022) and ± 7.34 μmol kg^{-1} (2023), while Ni are 0.11 - 0.18 μg L^{-1} and are too small to resolve on the plots.

Discussion

mERW with olivine can increase the levels of olivine dissolution products (e.g., alkalinity and trace metals) in sediment porewater and in turn, impact benthic species. Local changes to alkalinity related to mERW may benefit shellfish growth through greater availability of carbonate and bicarbonate ions, enabling shellfish to more readily form calcium carbonate[12]. Notably, porewater TA was highest at the Olivine treatment site at the start of the experiment (Fig. 4A). As such, the slightly higher biomass of oysters at the Olivine treatment site, compared to Control treatments, 64 days post-placement could be due to these favorable environmental conditions. Alternatively, oyster growth can be impacted by food availability. Recent research has found that OAE-induced changes in seawater composition might influence primary producers and thus available food sources. Hutchins et al. 2023[30] showed that two diatom species utilized Si and Fe from a synthetic olivine leachate to achieve near-maximum growth rates. However, probably because of nitrogen (N) limitation at the study site, Guo et al. 2024[31] found no positive effects of olivine dissolution on the growth of diatoms and other phytoplankton. When testing only alkalinity enhancement effects on phytoplankton, no effects were observed on communities[32] or species viability and growth rate[33] and when testing both Si and calcium (Ca)-based OAE, a limited effect was reported for diatom silicification[34]. We did not observe increased food levels resulting from olivine, as surface sediment total organic carbon (TOC) concentrations and water column chlorophyll *a* levels remained consistent across all treatments in the first two months after olivine placement (Fig. S3.4 - S3.5). The lack of effect was likely because there was no measurable increase in bottom water concentrations of olivine dissolution products. Taken together, it is unlikely that the higher oyster biomass at the Olivine treatment site was a result of increased food availability.

Furthermore, given that Olivine treatment oysters had the highest biomass following the period with the highest porewater trace metal concentrations, it does not appear that the porewater metals negatively affected oyster growth, or at least that any negative effect was counteracted by the positive effect of simultaneously increased porewater alkalinity concentrations. This finding is supported by bioconcentration factor (BCF) estimates (see Methods). Oysters from the Olivine treatment demonstrated consistently lower Ni BCF values across all dates (e.g., 131 ± 91 SD on day 64, as compared to >1000 for all other treatments, Table S1), indicative of an overall lower susceptibility to Ni accumulation.

With regards to trace metal bioaccumulation, one unexpected finding of this study is that Control West oysters had the highest Ni, Cr, and Co body burden after 64 days of exposure (Fig. 3) even though the Olivine treatment site had the highest Ni, Cr and Co porewater concentrations during this period (Fig. 4, S1.1). Moreover, on the same date, the Control West oysters exhibited the highest BCF for Ni (5625 ± 1935) of any treatment during the experiment (Table S1). Bioaccumulation of metals in marine bivalves occurs when they accumulate metals at rates greater than the loss rates, and these are a function of assimilation efficiencies of ingested metals, absorption of dissolved metals, and depuration processes that are dependent on metabolic processes[35,36]. At the beginning of the experiment, Control West porewaters had lower salinity (Fig. S3.1) and higher concentrations of sulfide than other treatments (Fig. S3.2). Oysters are susceptible to sulfide exposure, which can increase their vulnerability to environmental stressors by affecting detoxification mechanisms[37,38]. Furthermore, low salinity conditions can increase bioavailability and accumulation of some trace metals due to changes in free ion activity[39,40]. Therefore, unfavorable environmental conditions may have impacted Control West oyster bioaccumulation and detoxification processes and contributed to their relatively high Ni body burden. Additionally, oysters can accumulate dissolved metals through their gills[41], and through branchial filtration by assimilating ingested particulate organic matter and phytoplankton[42,43]. Here, analyses of sediment grain size indicate net movement of fine-grained material from the east to the west, from the Olivine treatment towards the Control West treatment (Fig. S3.3). Thus, Control West oysters may have had relatively high metal assimilation compared to other treatments due to higher exposure to, and filtration of, very fine grained olivine particles which then dissolved in the digestive system. Ultimately, a few mechanisms could account for the increased metal accumulation of Control West oysters, as compared to other sites, despite Control West porewaters having lower concentrations of olivine-derived dissolved metals in the first few months of the experiment.

Importantly, despite the comparatively high concentration of metals in Control West oysters at the beginning of the experiment, these concentrations decreased through time while the biomass of Control West oysters increased, as did the oyster biomass at all treatments. Therefore, the early accumulation of trace metals at Control West did not cause a long-term negative physiological impact, as oyster biomass was not statistically different from other treatments 147 and 300 days after olivine placement. In addition, the bioconcentration factor for Ni, Cr, and Co decreased with time suggesting a decline in metal assimilation or efficient detoxification of metals (Table S1, e.g., Ni BCF on September 7, 2022 was 5625 ± 1935 SD vs. 1735 ± 393 on May 10, 2023). An experimental study on *Crassostrea hongkongensis* (Lam & B. Morton, 2003) noted a high turnover rate for Ni in oysters, where Ni in oyster tissue reached a steady state after one week of exposure and maintained low concentrations, likely due to regulation mechanisms such as sequestration by metallothionein-like proteins[41]. More than 90% of Ni accumulated in oysters during a 4-week exposure under laboratory conditions, as well as in oysters from a contaminated estuary, were eliminated within a few weeks of depuration[41,44]. In the present study, we suggest that natural olivine transport and redistribution decreased the overall pool of olivine grains and dissolved metals throughout the project area and allowed for depuration/detoxification to occur. In addition, assimilation efficiencies of diverse metals, including Co, from ingested phytoplankton and subsequent efflux rates in *C. virginica* were generally comparable to those in the clams *Macoma balthica* (Linnaeus, 1758) and *Mercenaria mercenaria* (Linnaeus, 1758) and in the blue mussel *Mytilus edulis* (Linnaeus, 1758)[43], suggesting that other bivalves would likely respond similarly to olivine as oysters.

Global Context

While the current study is the first marine application of olivine for the purpose of carbon removal, olivine was previously applied as a 30 cm layer to a small section of Kirkebukten port, Bergen, Norway, to assess its potential for pollution adsorption. In that project, mussels were placed in bags and exposed to olivine for 12 weeks. The mussels ultimately accumulated between 0.5 and 1.0 μg Ni g dw^{-1} [45], while naturally occurring mussels collected from the site 4 years after olivine placement accumulated between 1.3 and 3.5 μg Ni g dw^{-1} [26]. These accumulation levels are comparable to the current study (Fig. 5), where only oysters from the Control West treatment, 64 days post-olivine placement, exhibited higher Ni accumulation (maximum 5.2 μg Ni g dw^{-1}). Additionally, mussels from the Norwegian experiment accumulated similar to higher amounts of Cr (0.5 to 4.1 μg Cr g dw^{-1}) compared to oysters in the current study (0.1 to 0.6 μg Cr g dw^{-1}). Thus, the magnitude of metal bioaccumulation measured in this study appears to be representative of bivalves under field olivine exposure. Bivalves have also been exposed to olivine in a laboratory setting. Bent-nosed clams (*Macoma nasuta,* Conrad, 1837) accumulated 6.8 μg Ni g dw^{-1} and 0.09 μg Cr g dw^{-1}, with no Co accumulation[24] (wet weight to dry weight conversion based on a 0.489 ratio for bivalves[46]) over 28 days of exposure in tanks. Thus, Ni accumulation in clams under laboratory conditions reached slightly higher levels than oysters from the current study over 64 days of field exposure. These findings suggest that species with different feeding types and behaviors may respond differently to olivine exposure, and that laboratory experiments may overestimate effects, potentially due to limited water exchange and dilution, as compared to field conditions.

In general, researchers and regulators have extensively studied oysters due to their commercial importance in aquaculture and food production. The maximum acceptable Ni concentration in shellfish published by the National Shellfish Sanitation Program, US Food and Drug Administration, is 80 μg g dw^{-1} [47]. According to the Norwegian classification of environmental contamination level based on metal body burden in mussels, Ni concentrations < 5 μg g dw^{-1} are regarded as the lowest condition class contamination level[48]. The oyster Ni accumulation measured in the current study is at or below established warning thresholds. The Ni and Cr body burden concentrations are also well within the range of values published for bivalves from natural settings (Fig. 5). Therefore, mERW with olivine sand had a limited effect on trace metals bioaccumulation in oysters and does not appear to be problematic for human consumption and the shellfish industry.

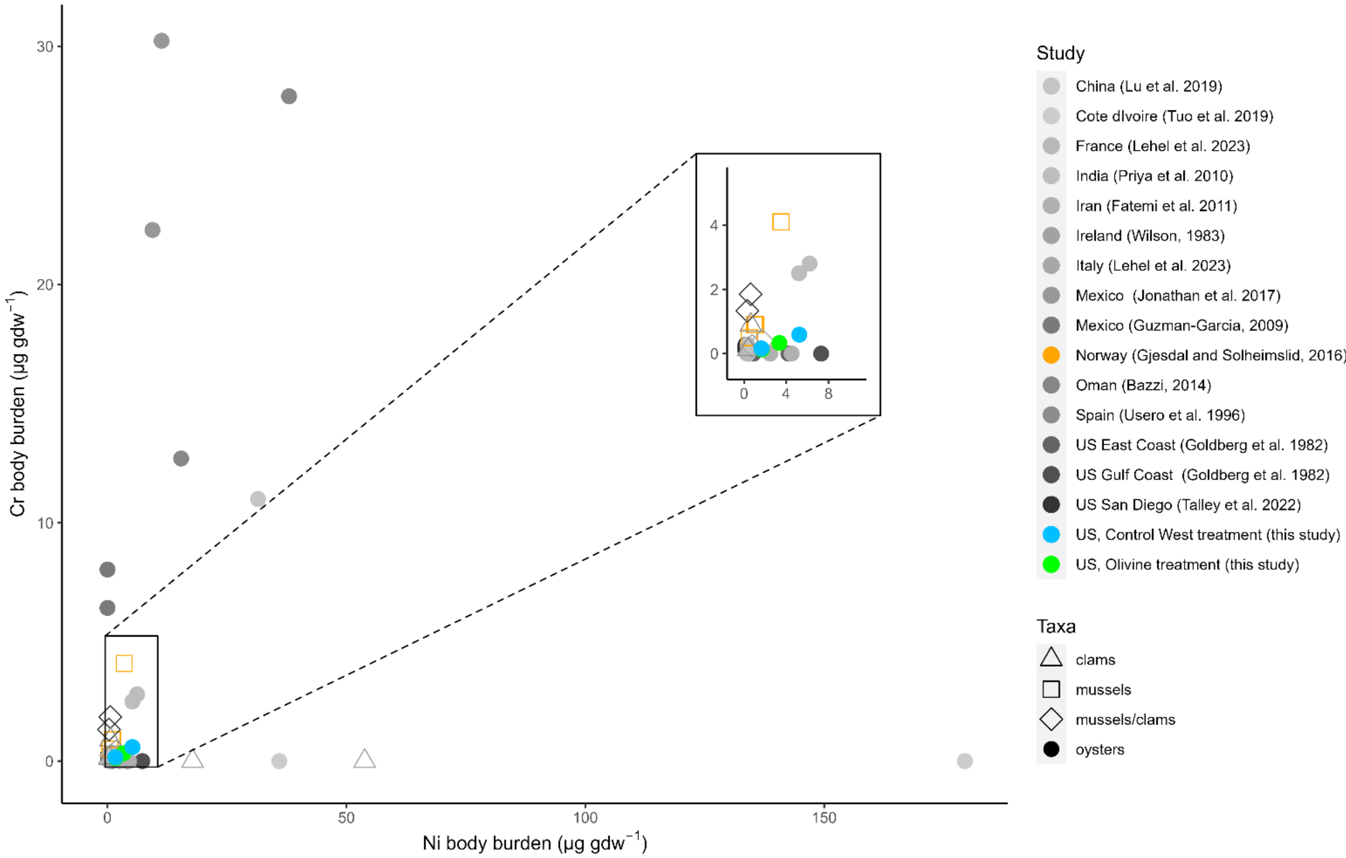

Fig. 5 Comparison of mean Ni and Cr body burden (μg g dw^{-1}) in oysters and other bivalves measured in the current study and other studies worldwide (underlying data presented in Table S2). Norway data points represent results for mussels exposed to olivine in Kirkebukten port, Bergen, Norway.

Future Work

The results of this study suggest that oyster growth is positively affected by olivine exposure, potentially related to increased alkalinity concentrations resulting from olivine dissolution, however, this effect was not strong and was only observed in the first 64 days after olivine placement, and thus requires further testing. The results of this study also indicate limited impact of olivine-derived metals on juvenile and adult oysters, but future work should include testing of different life stages (e.g. oyster larvae) which may be more sensitive. Further field tests should also encompass other benthic species with varied functional traits, including those that inhabit sediment, burrow, and act as deposit feeders. These organisms would be directly exposed to olivine sand and its dissolution products in porewaters. Crucially, future research should also prioritize field experiments across diverse environmental conditions, as numerous factors influence the speciation and bioavailability of metals. Special attention might be given to bioaccumulation effects under low salinity, low oxygen and high sulfide conditions. These field studies should be accompanied by controlled lab experiments to help disentangle competing biogeochemical processes. Furthermore, this study deployed olivine sand within the Peconic Bay, NY, a partially enclosed, low-energy system. Testing high-energy, open-ocean coastal areas will likely reveal additional insights, such as the impact of high porewater advection and dilution rates, as well as rapid sediment redistribution. Such insights will be instrumental in determining if, how and when mERW projects can be implemented safely, paving the way for effective and responsible climate intervention strategies in marine ecosystems.

Materials and methods

Experiment design and field site

The field trial was located at a beach adjacent to the North Sea Beach Colony along the southern shore of Little Peconic Bay in Southampton, New York, USA (40.947886°, -72.427809° (ESPG:4326)). The bay forms part of the larger Peconic Bay tidal estuary system, situated between the north and south forks of eastern Long Island. The system is fed by the Peconic River in the west, and is separated from the Atlantic Ocean to the east by a series of islands, sounds and tidal channels. The site is tidally dominated, having a tidal range of 0.87 m[49] and strong localized tidal currents that run through the channels between landmasses. The strongest currents flow at rates of up to 1.2 m/s through the channel between Cow Neck and Robins Island, which separates Little Peconic Bay from Great Peconic Bay[50]. The islands to the east of the bay, including Shelter Island and Gardiners Island, provide protection from incoming waves and swells that originate in the Atlantic Ocean. Internally generated waves are fetch-limited, forming short-period, small-amplitude wind-waves; these types of waves can be short and steep and have erosive power along beaches. The water temperature is seasonally variable, peaking at an average of 25°C in July and dropping to 3.9°C in January as recorded at the Shelter Island USGS Station (01304650)[51]. Generally, the Peconic Bay estuary has benthic fauna typical for sandy sediments of the temperate zone[52], and specifically in the project area there are no natural oyster beds observed, although oyster aquaculture operates nearby.

From July 5th to July 8th, 2022, approximately 650 tonnes of mERW olivine sand was placed as a layer in the intertidal area of the North Sea Beach by Vesta, PBC. The sand was tailored to match the native grain size of the site, with a median grain size of 0.49 mm (D_{50}) and a fines content of 0.5% (<0.0625 mm). The sand used for this experiment was dunite rock, with a mineralogical composition consisting of 85 wt% forsteritic olivine, 6.7 wt% orthopyroxene, 5.2% chlorite, and minor fractions of serpentine and talc. However, throughout the text we refer to this sand simply by its primary mineral component, olivine. Mineralogical analyses of the sand were conducted at QMineral (Leuven, Belgium) using x-ray diffraction (XRD) on a Bruker D8 Advance with XE-T detector and Cu-Kα radiation. Spectra were interpreted using in-house software.

Four stations representing four treatment areas (Control West, Olivine, Control East 1, Control East 2) were chosen for the oyster experiment and to monitor porewater composition and sediment characteristics. The porewater sampling locations were within 40 m of the oyster plots in all treatment areas and remained fully submerged at mean low water by approximately ~ 0.5 m. The oyster bags at the olivine treatment site were located within the original footprint of the olivine deployment although wave and tidal energy reworked, and redistributed, the olivine over a larger area through time (Fig. 1).

Oyster field and laboratory methods

Eastern oysters (*C. virginica*) were purchased from a local commercial oyster farmer in Mastic Beach, NY. 80 juvenile oysters (of size 3-4 cm) were placed in marine grade plastic oyster bags (100 cm x, 50 cm with 14 mm mesh size), which were then secured sub-tidally with screw anchors. Four oyster bags were placed within each of the respective control and treatment areas (n=16) on July 14, 2022. Oyster bags were marked with buoys to discourage poaching and prevent injury to swimmers. Oyster maintenance occurred 1-2 times per week, and involved flipping each bag over to rotate the side facing the substrate, shaking and breaking apart attached oysters, and removing any fouling or debris attached to the mesh. Three (3) oysters were collected from each bag on September 7th, 2022 (64 days after olivine nourishment), November 29th, 2022 (105 days after olivine nourishment), and May 10th, 2023 (300 days after olivine nourishment). In each case, samples were transported back to the laboratory, and depurated in a holding tank with filtered seawater (salinity= 30 psu, temp= 20°C) for 24 hours. Soft tissue was dissected (using non-metallic scalpels) from shells, wet weights were recorded, and tissue was placed in a drying oven (60°C) for 2 days. Dry weights were then taken and the dried tissue was pulverized using a ceramic mortar and pestle, placed into falcon tubes and shipped to Dartmouth College, NH Trace element Analysis Core for trace metals analysis. Oyster tissue was sub-sampled (ca. 250 mg sample) into 50 ml polypropylene tubes and 5 ml of 9:1 HNO_3:HCl was added and the samples were left to 'cold digest' overnight. Samples were then digested in a MARS 6 (CEM, Matthews, NC) at 105°C with a 15-minute ramp and 45-minute hold. After cooling, 100 ul of H_2O_2 was added to each sample and the samples were heated again. Finally, samples were diluted to 50 ml. The digestion included blanks and standard reference materials (NIST 2976, mussel tissue and 1566b Oyster tissue) at a frequency of one each per 20 samples. All measurement steps were recorded gravimetrically. The sample digestates were analyzed by triple quadrupole ICP-MS (Agilent 8900, Wilmington, DE). The analyte suite included Al, V, Cr, Mn, Fe, Co, Ni, Cu, Zn, As, Se, Sr, Mo, Ag, Cd, Sn, Sb, Hg, Tl, Pb, U. All analytes were analyzed in He gas mode and Cr, V, As, Se, Cd were also analyzed in O_2 gas mode. The ICP-MS was calibrated with NIST-traceable standards (Inorganic Ventures, Christiansberg, VA) and second source standards used to create the calibration verification were run after every calibration and every 10 samples; recoveries were ca 100% +/- 5%. Average SRM recoveries for Cr, Co, Ni were: 87 +/- 7% (n=2 2976b only), 97 +/- 10% (n=6), 111 +/- 24% (n=6) respectively. Recoveries for Ni in 2976, where only a reference value is given, were biased high being 138 and 145% recovery of the reference value of 0.93 +/- 0.12; recoveries of Ni in 1566b (n=4), where its value is certified were 96 +/- 6%.

Sediment field and laboratory methods

Three sediment core surveys were conducted on August 16th, 2022, October 18th, 2022, and May 31st, 2023. Sediment cores were collected near oyster bag locations (Fig. 1) to a minimum depth of 20 cm and sub-sampled at depth horizons of 0-1, 1-3, 3-5, and 5-10 cm using an incremental sediment core extruder. Only the 1-3 cm sediment layer was analyzed for this study, based on the assumption that it was the most representative of the oyster environment as oyster bags were placed on the sediment surface. Sediment samples were stored in Whirlpak bags and dried at 60°C. The mineralogical composition of the samples was determined by XRD by QMineral as described above. Samples were homogenized with a mortar and pestle and dried to avoid a preferred orientation. In-house software was used for interpretation. Weight percent total organic carbon (TOC) from 1 - 3 cm was measured by the Arizona State University's Metals, Environmental and Terrestrial Analytical Laboratory (only for August and October 2022). Samples were sieved to remove particles >2 mm and milled to a fine powder. An aliquot of the milled sediment was then weighed into a silver capsule, fumigated with hydrochloric acid to remove carbonates, and dried at 60°C. Samples were analyzed on a Perkin Elmer Series II CHNS/O analyzer, calibrated using an acetanilide standard and Certified Reference Materials, TOC standard B2293 and NIST #2711. The precision of this method was approximately 0.03% TOC.

Additional sediment grab surveys were conducted in May, June, August, September, and October 2022, as well as June, August, and October 2023 to determine spatial and temporal variation in grain size distribution. Samples were collected with a 0.04 m^{-2} van Veen grab during each survey at seven transects throughout the study area, two stations per transect (Fig. S3.8). Following the methodology of Folk, 1974[53], samples were partitioned into three size-fractions by adding 50 ml of a 1% Calgon solution, mixing to disaggregate the particles in the sample, and wet sieving with distilled water through a combination of 2 mm and 63 μm sieves. The >2 mm and 2 mm-63 μm fractions were placed in a drying oven at 60°C for at least 48 hours to obtain dry weights. Water containing the <63 μm fraction (mud) was brought up to 1000 ml total volume in a graduated cylinder, mixed thoroughly, and subsampled with a 20 ml pipette at a depth of 20 cm, 20 seconds after mixing. Pipette samples were placed in a drying oven at 60°C for at least 48 hours to obtain dry weight estimates of the mud fraction. Mud weight estimates included a correction for the amount of Calgon added to the samples.

Sediment porewater and water column field and laboratory methods

Chlorophyll *a* was measured by sensor (In Situ Aqua TROLL 500) approximately 0.5 m above the seafloor concurrent with porewater surveys. Precision of the chlorophyll *a* sensor was 0.94 Relative Fluorescence Units (RFU). Seven porewater surveys were conducted throughout the experiment. Discrete porewater samples were collected via carbon fiber PushPoints (M. H. E. Products, East Tawas, MI) at 0 cm (i.e., water column, just above the sediment-water interface) and 2 cm. Approximately 40 mL of porewater was collected with a polycarbonate syringe, then filtered to 0.45 μm with a 13 mm diameter polyethersulfone syringe filter, and subsampled immediately on the beach. All protocols followed the best oceanographic sampling practices (Dickson et al., 2007). Porewater sub-samples were immediately taken back to the laboratory and either analyzed in-house or sent for external analyses. Conductivity was measured in-house using a Mettler Toledo Inlab Conductivity Probe. Salinity was calculated from conductivity using the algorithm of the Practical Salinity Scale of 1978[54,55]. The precision of this method was approximately 0.07 PSU. Nitrate+nitrite and ammonia were analyzed in the Gobler Laboratory at Stony Brook University using a Lachat Quikchem 8500 flow injection analyzer[56]. The precisions of these methods were approximately 0.14 and 0.16 μmol L^{-1}, respectively. Sulfide was measured following the Cline, 1969[57] method. The precision of this method was approximately 2.2 μmol L^{-1}. Trace metals were analyzed at the University of Southern Mississippi's Center for Trace Analysis. Trace metal samples were diluted 30-fold in ultrapure 0.16 M nitric acid (Fisher Optima) which contained approximately 17 nM indium as an internal standard. Diluted samples were measured by sector-field inductively coupled plasma mass spectrometry (ThermoFisher Element XR) using a Peltier spray chamber (PC3, Elemental Scientific) and low flow perfluoroalkoxy alkane nebulizer (Elemental Scientific). Cd and Pb were used for quantification in low resolution, with Mo monitored for correction of molybdenum monoxide interference on Cd. The other elements (Ni, Cr, Co, Al, Cu, and Zn) were determined in medium resolution to eliminate common isobaric interferences. Quantification utilized standard curves which contained 30-fold diluted, cleanly collected seawater, to eliminate matrix effects. To check accuracy, SLEW-4, an estuarine water Certified Reference Material (National Research Council Canada) was analyzed. However, because many of the certified values of SLEW-4 are lower than the concentration range of the samples, a laboratory-fortified aliquot of SLEW-4 was prepared. For Co, Cu, and Ni, the recovery of SLEW-4 was typically within 10% of the certified values. For all elements, the recovery of the fortified SLEW-4 was typically within 10% of the fortified analyte addition. The precision of this method were approximately 0.14 μg Ni L^{-1}, 0.016 μg Cr L^{-1}, 0.004 μg Co L^{-1}, 7.8 μg Al L^{-1}, 0.015 μg Cd L^{-1}, 0.6 μg Cu L^{-1}, 0.05 μg Pb L^{-1}, 2.9 μg Zn L^{-1}. Total alkalinity for the 2022 samples was analyzed by the Subhas Lab at Woods Hole Oceanographic Institute. Total alkalinity was determined using an open-system Gran titration on weighed 2.5 mL single samples, using a Metrohm 805 Dosimat and 855 robotic Titrosampler, calibrated twice daily against in-house seawater standard that was intercalibrated against Certified CO_2 in Dickson Seawater Reference Material (Scripps Institution of Oceanography). The precision of this method was approximately 4.4 μmol kg^{-1}. Total alkalinity for the one timepoint in 2023 was determined in-house using a Metrohm 855 Robotic Titrosampler and 805 Dosimat system following the procedures detailed in Dickson et al. (2003) with modifications for small volume samples. These included a salinity adjusted (0.7M sodium chloride) ~0.01N hydrochloric acid solution dispensed at 5 μL intervals into a ~3 mL seawater sample. Certified CO_2 in the Dickson Seawater Reference Material (Scripps Institution of Oceanography) was titrated in triplicate before and after every 15 samples and a linear Gran function was applied to estimate the equivalence point in both sample and standards. The precision of this method was approximately 7.3 μmol kg^{-1}.

Statistical analysis of oyster data

Differences in the selected trace metals (Ni, Cr, Co) concentration in the oyster tissue, as well as oyster dry weights among treatments and dates, were tested using a generalized linear mixed model (GLMM) based on a normal distribution. The model included 2 fixed factors (Treatment, Date), their interaction, and a random factor that represented the bag in which oysters were kept. The best model was selected according to Akaike's Information Criterion and diagnostic tests such as dispersion, residuals, and Levene tests for heteroscedasticity following DHARMa R package (version 0.4.6). When significant effects were detected by the main test, Tukey pairwise tests were applied at a family error rate of 0.05. All analyses were performed in R[58] using the 'glmmTMB' package, version 4.2.2.

Bioconcentration factor (BCF) which represents the degree of metal concentration in an organism was calculated for Ni, Cr, and Co using the formula:

$$BCF = \frac{Cm}{Cw}$$

Where Cm is the metal concentration in an organism's tissue expressed as μg g^{-1} dry weight, and Cw is the metal concentration in water expressed as μg mL^{-1}. To account for oysters exposure to a range of metal concentrations with time, BCF for oyster samples collected on September 7, 2022, was calculated using the average metal concentration in the bottom water and porewater measured between July 15 and August 2, 2022; for oysters collected on November 29 2022 using the average metal concentration in the porewater measured between July 15 and October 10 2022; while for oysters collected in and May 10, 2023, using the average metal concentration in the porewater measured between July 15, 2022, and May 31, 2023.

Acknowledgments

The authors would like to acknowledge Ryan Hostak, Sydney Ethen, Hannah van de Mortel, Ocea S. van Loenen, George Monez, Rebecca Holloway, Mark Jacobello, Damien Crowley, Noah Feigenbaum, Avery Testa, Tatiana Markuou and Sophie Walkenhorst for their help with sediment and porewater sampling fieldwork; as well as Joseph Costanzo, Stephen Havens, Kaitlin Morris, Jordan Russo, Eleanor Evans and Virginia Gilliland for field and assistance with oyster sampling. The authors thank Juan Alberti and Mikołaj Mazurkiewicz for their help with data analysis. The authors also acknowledge Aram Terchunian and First Coastal Corp for assistance in establishing the field trial and monitoring program and thank Guido Schattanek, the North Sea Beach Colony community and the Town of Southampton, NY for their support.

References

1. National Academies of Sciences, Engineering, and Medicine. *A Research Strategy for Ocean-Based Carbon Dioxide Removal and Sequestration*. https://doi.org/10.17226/26278 (2022).
2. Cross, J. N. *et al. Strategy for NOAA Carbon Dioxide Removal Research: A White Paper Documenting a Potential NOAA CDR Science Strategy as an Element of NOAA's Climate Mitigation Portfolio*. 65 (2023).
3. Geerts, L. J. J., Hylén, A. & Meysman, F. J. R. Review and syntheses: Ocean alkalinity enhancement and carbon dioxide removal through marine enhanced rock weathering using olivine. *Biogeosciences* **22**, 355–384 (2025).
4. Campbell, J. S. *et al.* Geochemical Negative Emissions Technologies: Part I. Review. *Frontiers in Climate* **4**, (2022).
5. Meysman, F. J. R. & Montserrat, F. Negative CO_2 emissions via enhanced silicate weathering in coastal environments. *Biol. Lett.* **13**, 20160905 (2017).

6. Renforth, P. & Henderson, G. Assessing ocean alkalinity for carbon sequestration. *Reviews of Geophysics* **55**, 636–674 (2017).
7. Feng, E. Y., Koeve, W., Keller, D. P. & Oschlies, A. Model-Based Assessment of the CO2 Sequestration Potential of Coastal Ocean Alkalinization. *Earth's Future* **5**, 1252–1266 (2017).
8. Palmiéri, J. & Yool, A. Global-Scale Evaluation of Coastal Ocean Alkalinity Enhancement in a Fully Coupled Earth System Model. *Earth's Future* **12**, e2023EF004018 (2024).
9. Bach, L. T., Gill, S. J., Rickaby, R. E. M., Gore, S. & Renforth, P. CO2 Removal With Enhanced Weathering and Ocean Alkalinity Enhancement: Potential Risks and Co-benefits for Marine Pelagic Ecosystems. *Frontiers in Climate* **1**, (2019).
10. IPCC. *Global Warming of 1.5°C: IPCC Special Report on Impacts of Global Warming of 1.5°C above Pre-Industrial Levels in Context of Strengthening Response to Climate Change, Sustainable Development, and Efforts to Eradicate Poverty.* (2022).
11. Gazeau, F. *et al.* Impacts of ocean acidification on marine shelled molluscs. *Mar Biol* **160**, 2207–2245 (2013).
12. Waldbusser, G. G. *et al.* Saturation-state sensitivity of marine bivalve larvae to ocean acidification. *Nature Clim Change* **5**, 273–280 (2015).
13. Schwaner, C., Barbosa, M., Pales Espinosa, E. & Allam, B. Probing the role of carbonic anhydrase in shell repair mechanisms in the eastern oyster *Crassostrea virginica* under experimental acidification stress. *Journal of Experimental Marine Biology and Ecology* **572**, 151990 (2024).
14. Clements, J. C. & Chopin, T. Ocean acidification and marine aquaculture in North America: potential impacts and mitigation strategies. *Reviews in Aquaculture* **9**, 326–341 (2017).

15. Mangi, S. C. *et al.* The economic impacts of ocean acidification on shellfish fisheries and aquaculture in the United Kingdom. *Environmental Science & Policy* **86**, 95–105 (2018).
16. Townhill, B. L., Artioli, Y., Pinnegar, J. K. & Birchenough, S. N. R. Exposure of commercially exploited shellfish to changing pH levels: how to scale-up experimental evidence to regional impacts. *ICES Journal of Marine Science* **79**, 2362–2372 (2022).
17. FAO. *The State of World Fisheries and Aquaculture 2022. Towards Blue Transformation.* https://doi.org/10.4060/cc0461en (2022).
18. Hu, X. & Cai, W.-J. An assessment of ocean margin anaerobic processes on oceanic alkalinity budget. (2011).
19. Bristow, L. A., Mohr, W., Ahmerkamp, S. & Kuypers, M. M. M. Nutrients that limit growth in the ocean. *Curr Biol* **27**, R474–R478 (2017).
20. Flipkens, G., Blust, R. & Town, R. M. Deriving Nickel (Ni(II)) and Chromium (Cr(III)) Based Environmentally Safe Olivine Guidelines for Coastal Enhanced Silicate Weathering. *Environ. Sci. Technol.* **55**, 12362–12371 (2021).
21. Montserrat, F. *et al.* Olivine Dissolution in Seawater: Implications for CO_2 Sequestration through Enhanced Weathering in Coastal Environments. *Environ. Sci. Technol.* **51**, 3960–3972 (2017).
22. Anacleto, P. *et al.* Effects of depuration on metal levels and health status of bivalve molluscs. *Food Control* **47**, 493–501 (2015).
23. Jeong, H., Byeon, E., Kim, D.-H., Maszczyk, P. & Lee, J.-S. Heavy metals and metalloid in aquatic invertebrates: A review of single/mixed forms, combination with other pollutants, and environmental factors. *Marine Pollution Bulletin* **191**, 114959 (2023).

24. Jankowska, E., Montserrat, F., Romaniello, S. J., Walworth, N. G. & Andrews, M. G. Metal bioaccumulation and effects of olivine sand exposure on benthic marine invertebrates. *Chemosphere* **358**, 142195 (2024).

25. Flipkens, G. *et al.* Acute bioaccumulation and chronic toxicity of olivine in the marine amphipod Gammarus locusta. *Aquatic Toxicology* **262**, 106662 (2023).

26. Gjesdal, A. & Solheimslid, S. O. *Environmental Condition in Kirkebukten. Monitoring Results 2015*. 36 (2016).

27. O'Connor, T. P. National distribution of chemical concentrations in mussels and oysters in the USA. *Marine Environmental Research* **53**, 117–143 (2002).

28. Wang, W.-X., Meng, J. & Weng, N. Trace metals in oysters: molecular and cellular mechanisms and ecotoxicological impacts. *Environ. Sci.: Processes Impacts* **20**, 892–912 (2018).

29. Saili, K. S., Cardwell, A. S. & Stubblefield, W. A. Chronic Toxicity of Cobalt to Marine Organisms: Application of a Species Sensitivity Distribution Approach to Develop International Water Quality Standards. *Environ Toxicol Chem* **40**, 1405–1418 (2021).

30. Hutchins, D. A. *et al.* Responses of globally important phytoplankton groups to olivine dissolution products and implications for carbon dioxide removal via ocean alkalinity enhancement. *EGUsphere* 1–0 (2023) doi:10.1101/2023.04.08.536121.

31. Guo, J. A., Strzepek, R. F., Swadling, K. M., Townsend, A. T. & Bach, L. T. Influence of ocean alkalinity enhancement with olivine or steel slag on a coastal plankton community in Tasmania. *Biogeosciences* **21**, 2335–2354 (2024).

32. Ramírez, L. *et al.* Ocean Alkalinity Enhancement (OAE) does not cause cellular stress in a phytoplankton community of the sub-tropical Atlantic Ocean. *EGUsphere* 1–34 (2024) doi:10.5194/egusphere-2024-847.

33. Oberlander, J. L., Burke, M. E., London, C. A. & MacIntyre, H. L. Assessing the impacts of simulated Ocean Alkalinity Enhancement on viability and growth of near-shore species of phytoplankton. *EGUsphere* 1–21 (2024) doi:10.5194/egusphere-2024-971.

34. Ferderer, A. *et al.* Investigating the effect of silicate- and calcium-based ocean alkalinity enhancement on diatom silicification. *Biogeosciences* **21**, 2777–2794 (2024).

35. Fisher, N. S. & Reinfelder, J. R. *The Trophic Transfer of Metals in Marine Systems*. (In: Metal Speciation and Bioavailability in Aquatic Systems. A. Tessier and D.R. Turner, eds. John Wiley & Sons, 1995).

36. Wang, W.-X., Fisher, N. S. & Luoma, S. N. Kinetic determinations of trace element bioaccumulation in the mussel Mytilus edulis. *Marine Ecology Progress Series* **140**, 91–113 (1996).

37. Moullac, G. L. *et al.* Ecophysiological and Metabolic Adaptations to Sulphide Exposure of the Oyster Crassostrea gigas. *shre* **27**, 355–363 (2008).

38. Butterworth, K. G., Grieshaber, M. K. & Taylor, A. C. Behavioural and physiological responses of the Norway lobster, Nephrops norvegicus (Crustacea: Decapoda), to sulphide exposure. *Marine Biology* **144**, 1087–1095 (2004).

39. Rainbow, P. S. & White, S. L. Comparative strategies of heavy metal accumulation by crustaceans: zinc, copper and cadmium in a decapod, an amphipod and a barnacle. *Hydrobiologia* **174**, 245–262 (1989).

40. Wang, W.-X. & Rainbow, P. S. Influence of metal exposure history on trace metal uptake and accumulation by marine invertebrates. *Ecotoxicol Environ Saf* **61**, 145–159 (2005).

41. Yin, Q. & Wang, W.-X. Uniquely high turnover of nickel in contaminated oysters Crassostrea hongkongensis: Biokinetics and subcellular distribution. *Aquatic Toxicology* **194**, 159–166 (2018).

42. Rainbow, P. S., Smith, B. D. & Luoma, S. N. Differences in trace metal bioaccumulation kinetics among populations of the polychaete Nereis diversicolor from metal-contaminated estuaries. *Marine Ecology Progress Series* **376**, 173–184 (2009).

43. Reinfelder, J. R., Wang, W.-X., Luoma, S. N. & Fisher, N. S. Assimilation efficiencies and turnover rates of trace elements in marine bivalves: a comparison of oysters, clams and mussels. *Marine Biology* **129**, 443–452 (1997).

44. Wang, L. & Wang, W.-X. Depuration of metals by the green-colored oyster Crassostrea sikamea. *Environ Toxicol Chem* **33**, 2379–2385 (2014).

45. Sæterdal Bøyum, M. & Ane Moe, G. *Environmental Condition in Kirkebukten Monitoring Results 2019*. 54 (2020).

46. Gogina, M., Zettler, A. & Zettler, M. L. Weight-to-weight conversion factors for benthic macrofauna: recent measurements from the Baltic and the North seas. *Earth System Science Data* **14**, 1–4 (2022).

47. United States Food and Drug Administration. *National Shellfish Sanitation Program Guide for the Control of Molluscan Shellfish 2007 Revision.* 280 (2007).

48. The Norwegian Environment Agency (before the Norwegian Pollution Control Authority). *Guide for Classification of Environmental Quality in Fjords and Coastal Waters 2229/2007*. (2008).
49. NOAA. Datums for 8512735, South Jamesport NY. (2011).
50. Hardy, C. D. *A Preliminary Description of the Peconic Bay Estuary*. (1976).
51. USGS. Surface Water data for USA: USGS Surface-Water Monthly Statistics. (2024).
52. Cerrato, R. M., Flood, R. D. & Holt, L. C. *Benthic Mapping for Habitat Classification in the Peconic Estuary: Phase III Ground Truth Studies*. (2010).
53. Folk, R.L. (1974) Petrology of Sedimentary Rocks. Hemphill Publishing Co., Austin, 170 p. - References - Scientific Research Publishing. https://www.scirp.org/reference/referencespapers?referenceid=1471425.
54. Unesco. *The Practical Salinity Scale 1978 and the International Equation of State of Seawater 1980*. 25 (1981).
55. Unesco. *Algorithms for Computation of Fundamental Properties of Seawater*. 53 (1983).
56. Lachat. *Determination of Ammonia by Flow Injection Analysis, Quikchem Method 10-107-06-1-J.* (2008).
57. Cline, J. D. Spectrophotometric Determination of Hydrogen Sulfide in Natural Waters. *Limnology and Oceanography* **14**, 454–458 (1969).
58. R Core Team. R: A Language and Environment for Statistical Computing. R Foundation for Statistical Computing, Vienna (2024).

Supplementary Information

S1 Bottom water and porewater results for remaining trace metals

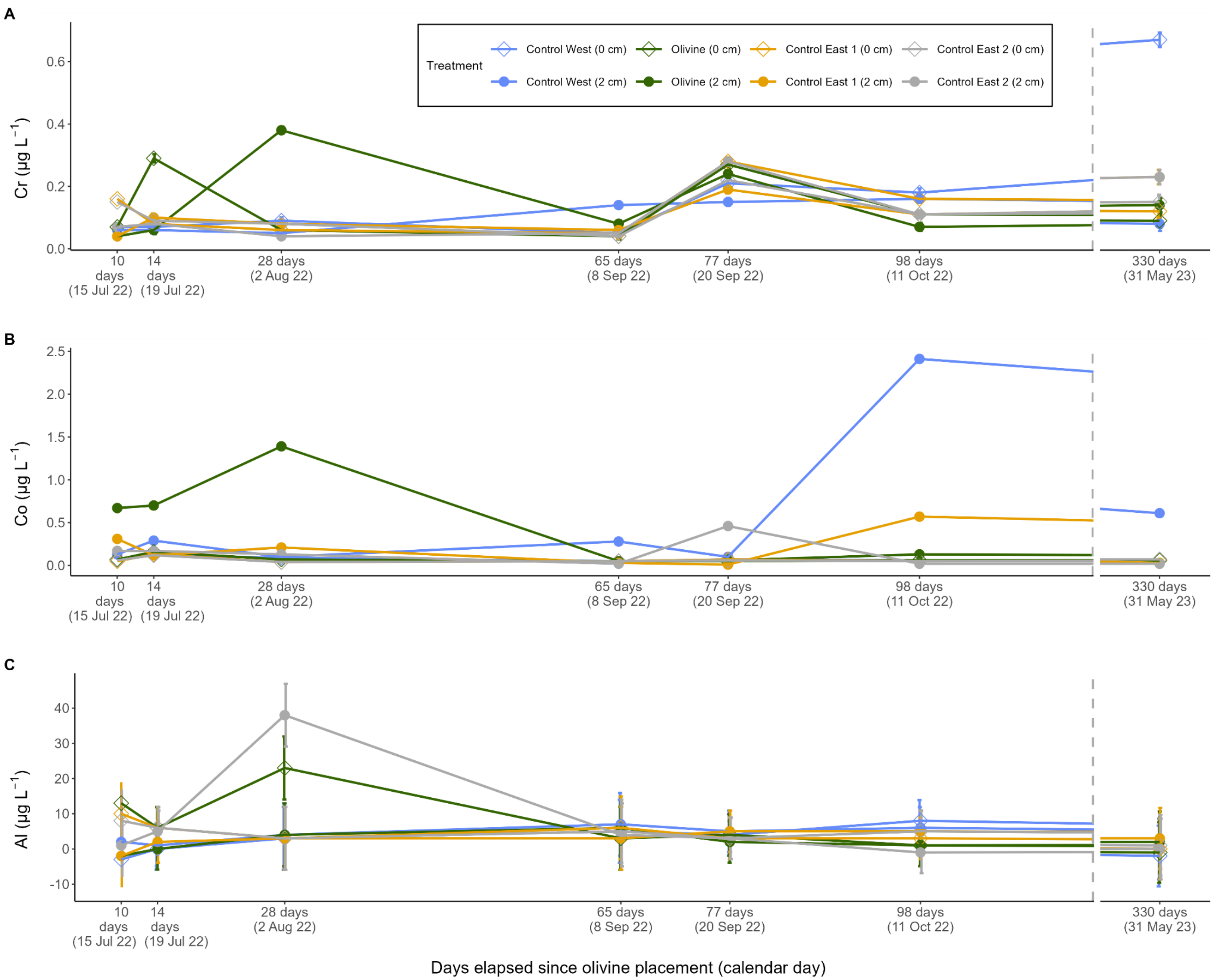

Fig. S1.1 A) Cr, B) Co, and C) Al concentration (µg L^{-1}) measured during the experiment in bottom water (0 cm) and porewater at 2 cm sediment depth. Colors represent four treatments, shapes represent bottom vs. porewater samples. ‘Jul’ stands for July, ‘Aug’ for August, ‘Sep’ for September, ‘Oct’ for October, ‘Nov’ for November. Analytical error bars for Co amounts 0.003 - 0.009 µg L^{-1} and are too small to resolve in the graphs.

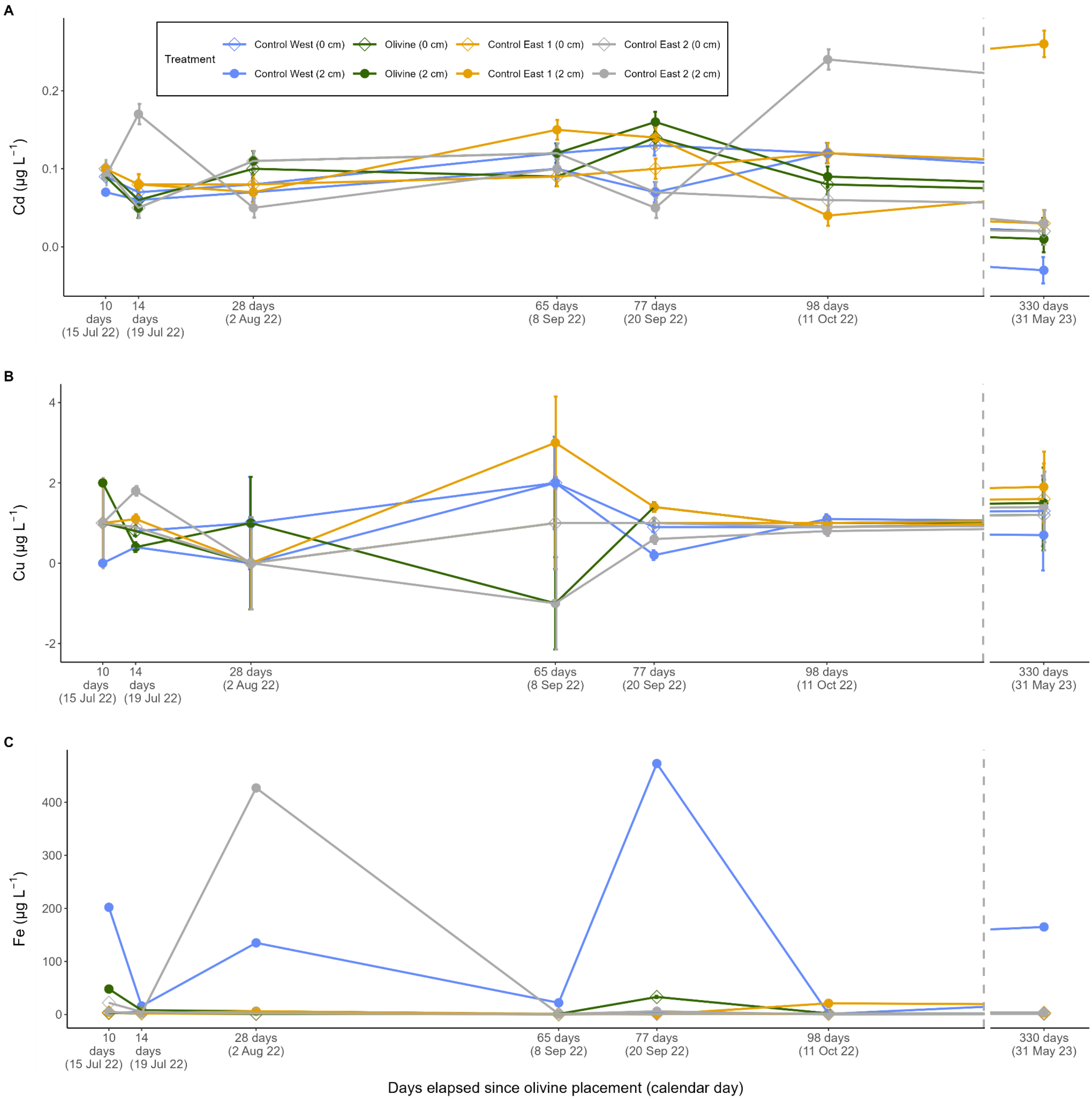

Fig. S1.2 A) Cd, B) Cu, and C) Fe concentration (µg L^{-1}) measured during the experiment in bottom water (0 cm) and porewater at 2 cm sediment depth. Colors represent four treatments, shapes represent bottom vs. porewater samples. 'Jul' stands for July, 'Aug' for August, 'Sep' for September, 'Oct' for October, 'Nov' for November. Analytical error bars for Fe amounts 1.2 - 1.9 µg L^{-1} and are too small to resolve in the graphs.

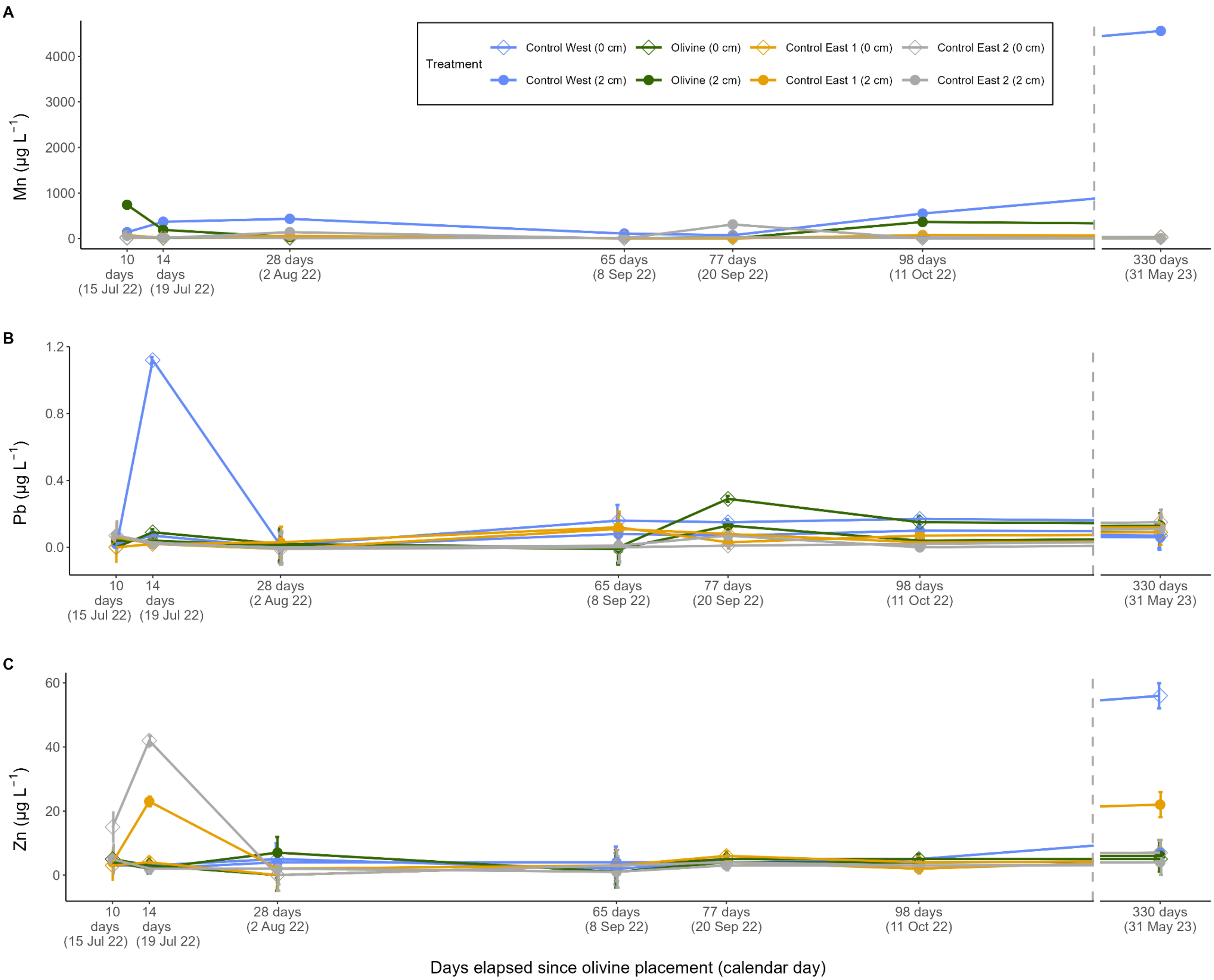

Fig. S1.3 A) Mn, B) Pb, and C) Zn concentration (µg L^{-1}) measured during the experiment in bottom water (0cm) and porewater at 2 cm sediment depth. Colors represent four treatments, shapes represent bottom vs. porewater samples. 'Jul' stands for July, 'Aug' for August, 'Sep' for September, 'Oct' for October, 'Nov' for November. Analytical error bars for Mn amounts 0.08 - 0.52 µg L^{-1} and are too small to resolve in the graphs.

S2 Oyster tissue body burden for remaining metals

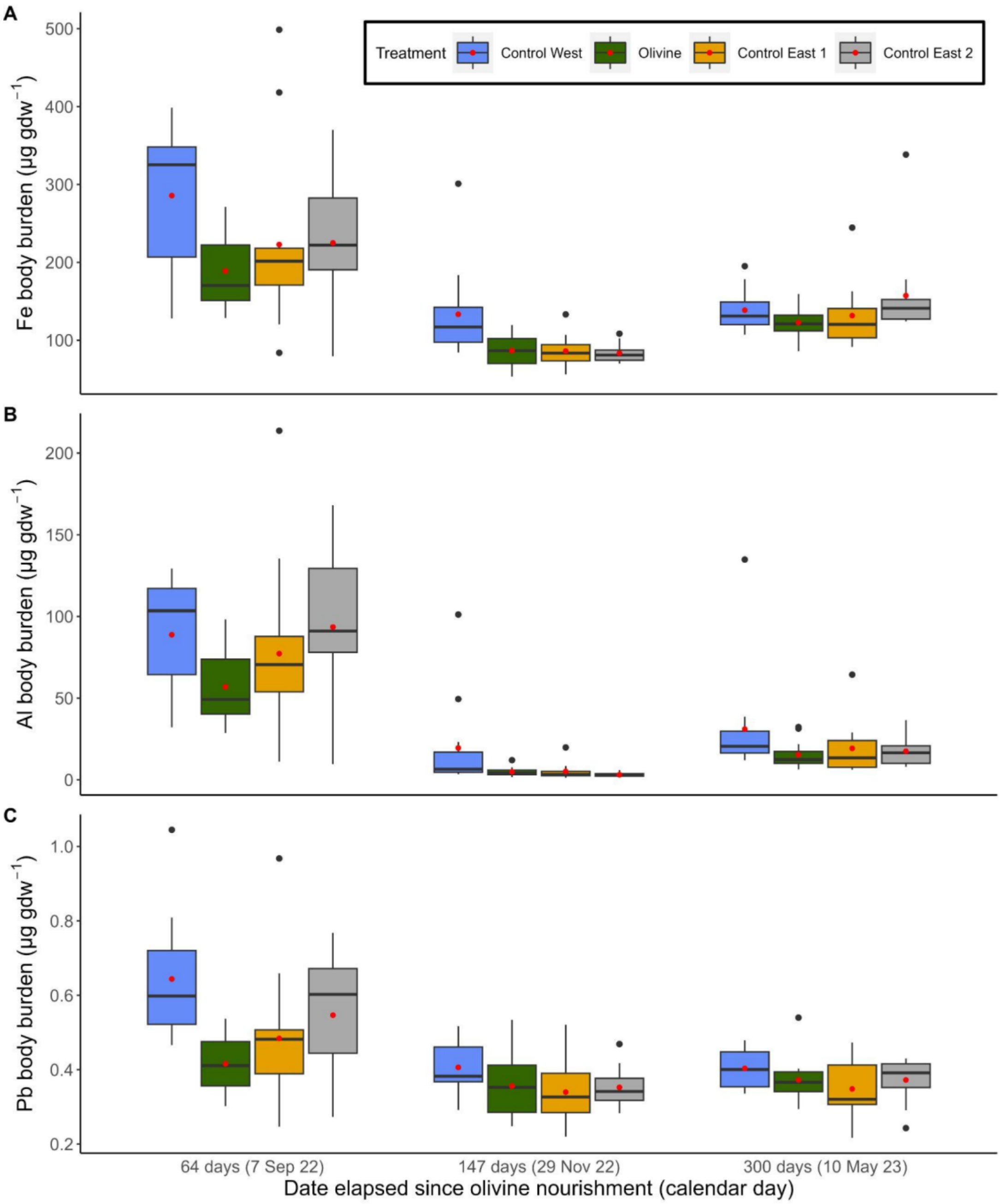

Fig. S2.1 Selected trace metals (A) Fe, B) Al, C) Pb oyster tissue body burden (µg g dw^{-1}) at four treatments and three sampling dates. Colors represent four treatments. Mean (red dot), median (horizontal line), 25th and 75th percentile (box), minimum and maximum value (vertical line), and outliers (black dot) are presented. 'Sep' stands for September, 'Nov' for November.

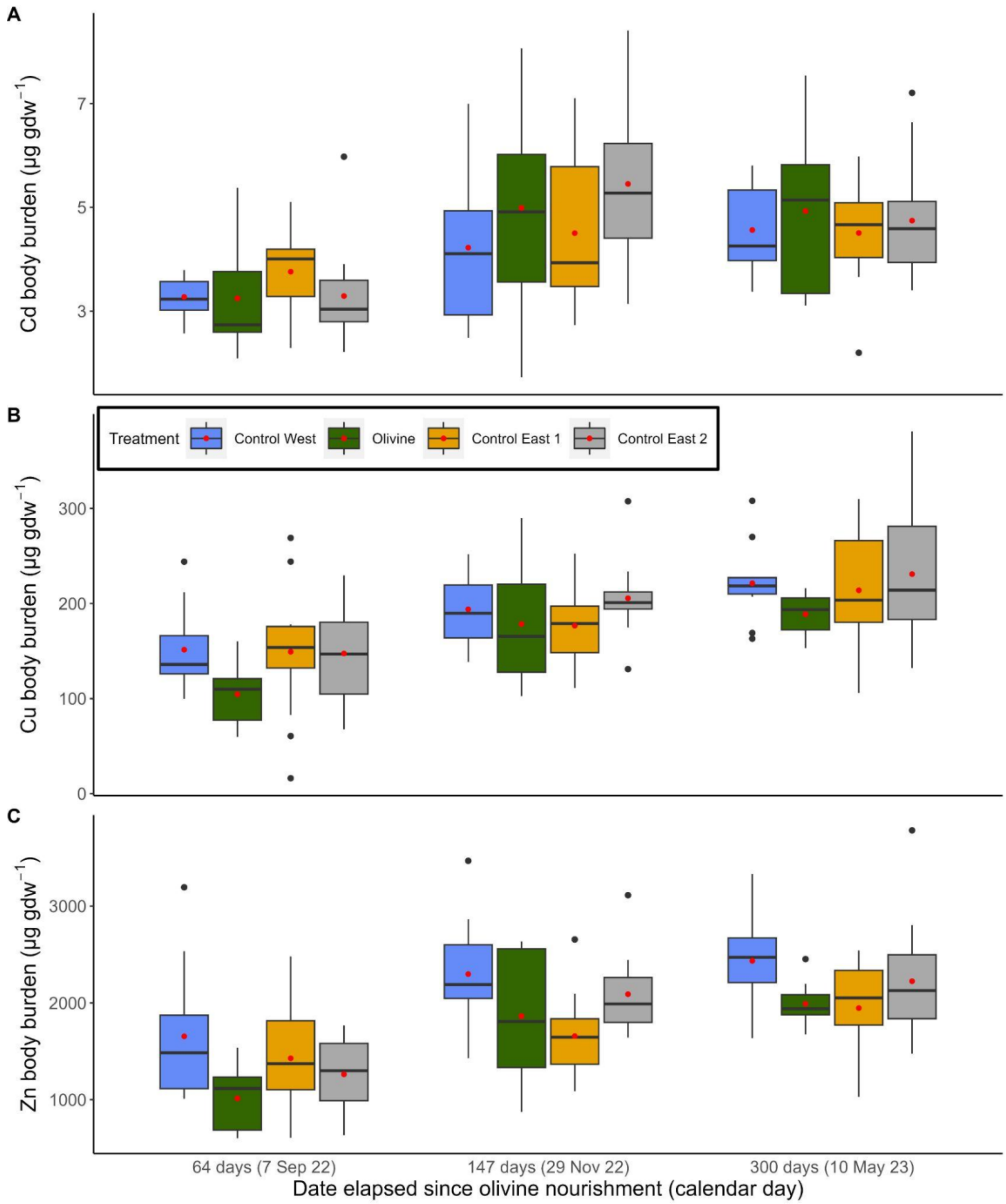

Fig. S2.2 Selected trace metals (A) Cd, B) Cu, C) Zn oyster tissue body burden (µg g dw^{-1}) at four treatments and three sampling dates. Colors represent four treatments. Mean (red dot), median (horizontal line), 25th and 75th percentile (box), minimum and maximum value (vertical line), and outliers (black dot) are presented. 'Sep' stands for September, 'Nov' for November.

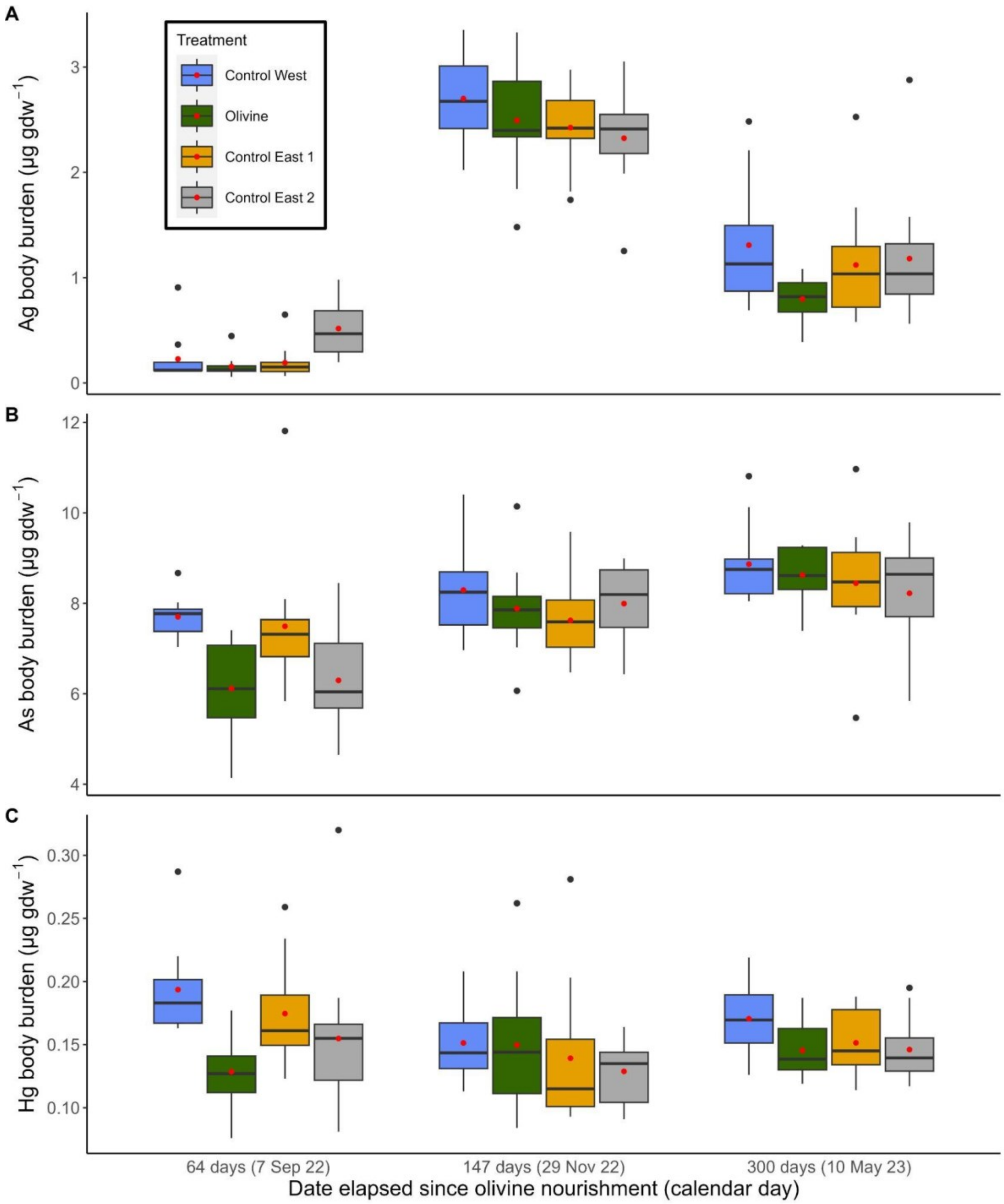

Fig. S2.3 Selected trace metals (A) Ag, B) As, C) Hg oyster tissue body burden (µg g dw^{-1}) at four treatments and three sampling dates. Colors represent four treatments. Mean (red dot), median (horizontal line), 25th and 75th percentile (box), minimum and maximum value (vertical line), and outliers (black dot) are presented. 'Sep' stands for September, 'Nov' for November.

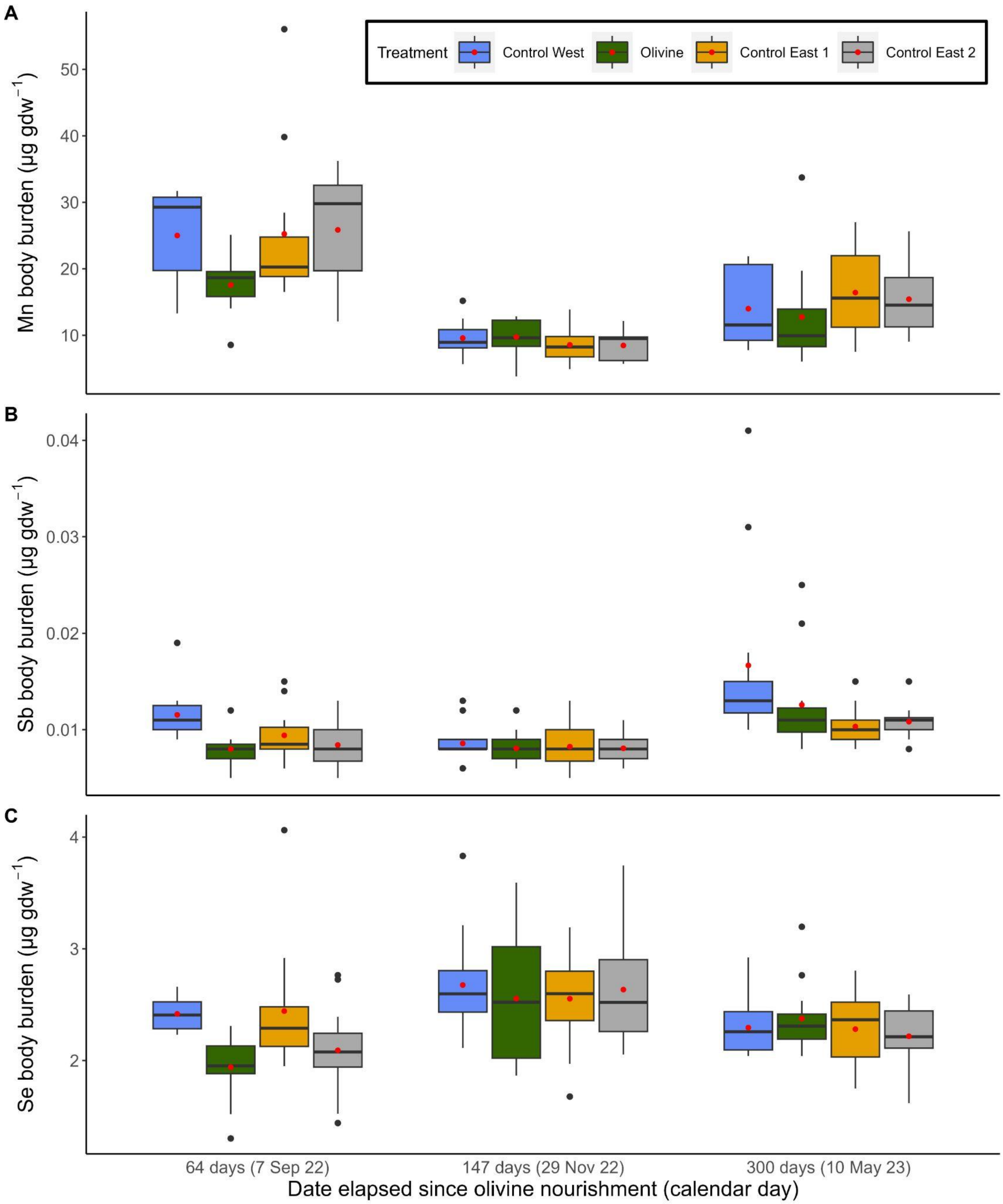

Fig. S2.4 Selected trace metals (A) Mn, B) Sb, C) Se oyster tissue body burden (µg g dw^{-1}) at four treatments and three sampling dates. Colors represent four treatments. Mean (red dot), median (horizontal line), 25th and 75th percentile (box), minimum and maximum value (vertical line), and outliers (black dot) are presented. 'Sep' stands for September, 'Nov' for November.

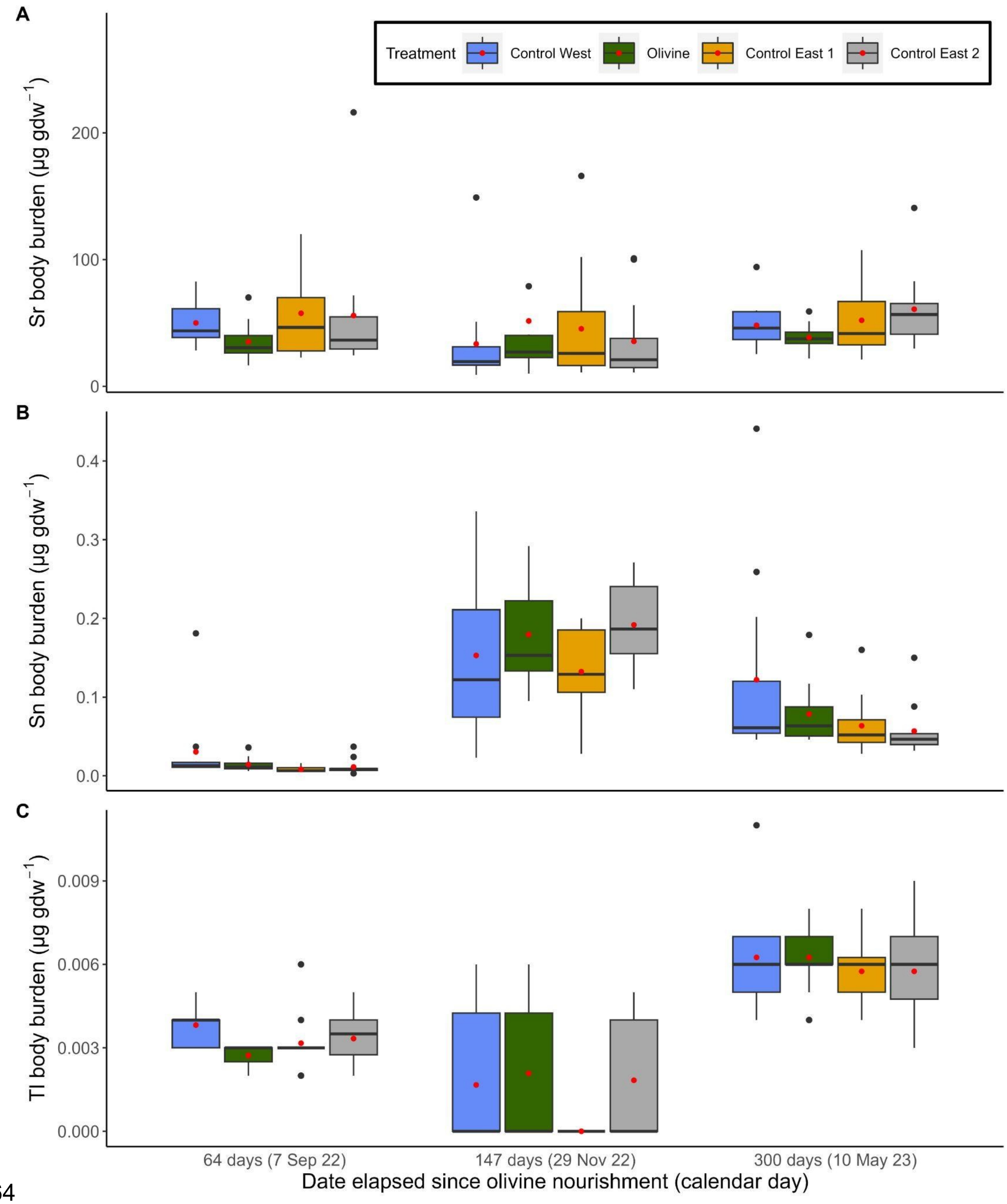

Fig. S2.5 Selected trace metals (A) Sr, B) Sn, C) Tl oyster tissue body burden (µg g dw^{-1}) at four treatments and three sampling dates. Colors represent four treatments. Mean (red dot), median (horizontal line), 25th and 75th percentile (box), minimum and maximum value (vertical line), and outliers (black dot) are presented. 'Sep' stands for September, 'Nov' for November.

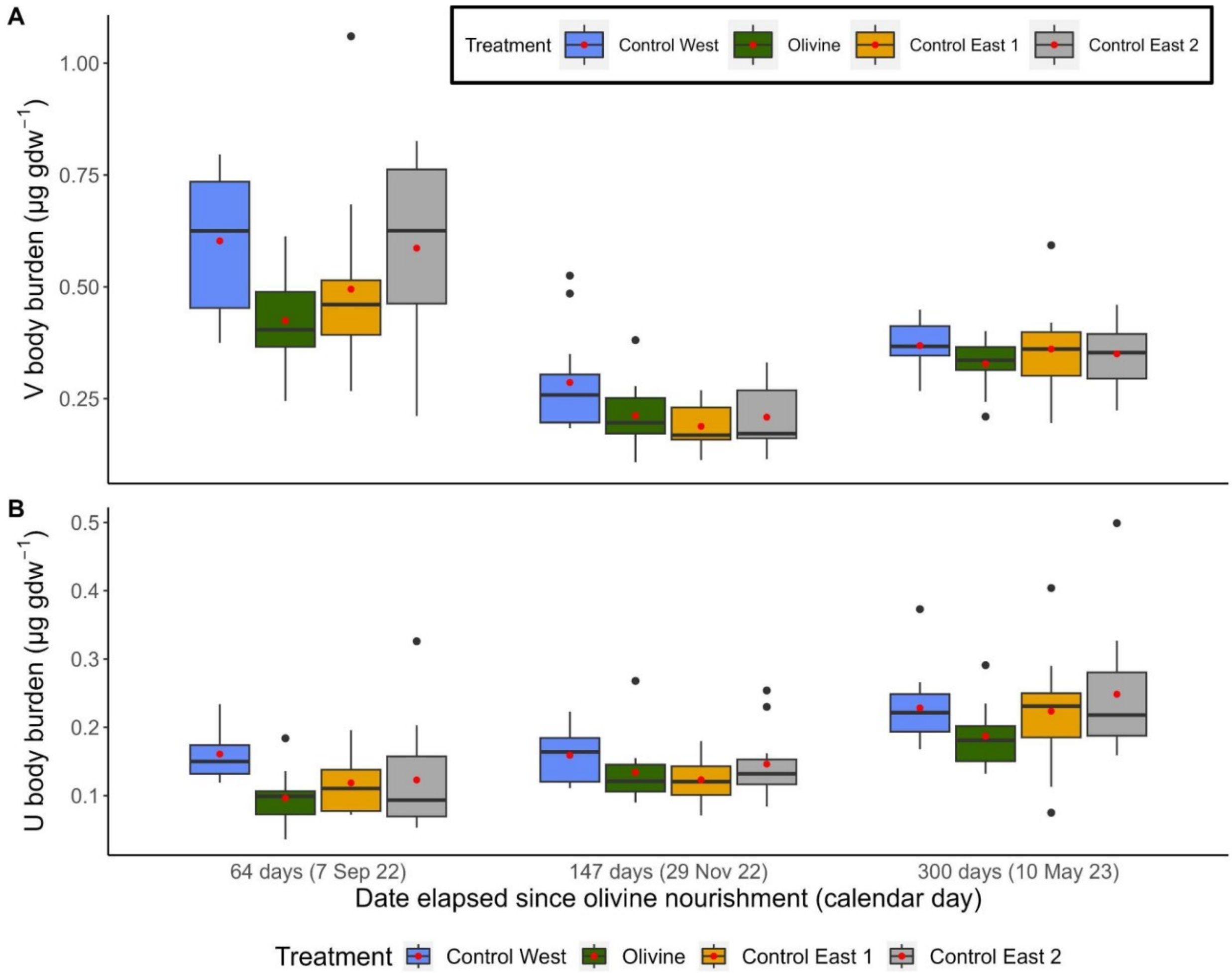

Fig. S2.6 Selected trace metals (A) V, B) U oyster tissue body burden (µg g dw^{-1}) at four treatments and three sampling dates. Colors represent four treatments. Mean (red dot), median (horizontal line), 25th and 75th percentile (box), minimum and maximum value (vertical line), and outliers (black dot) are presented. 'Sep' stands for September, 'Nov' for November.

S3 Background environmental parameters measured during the experiment

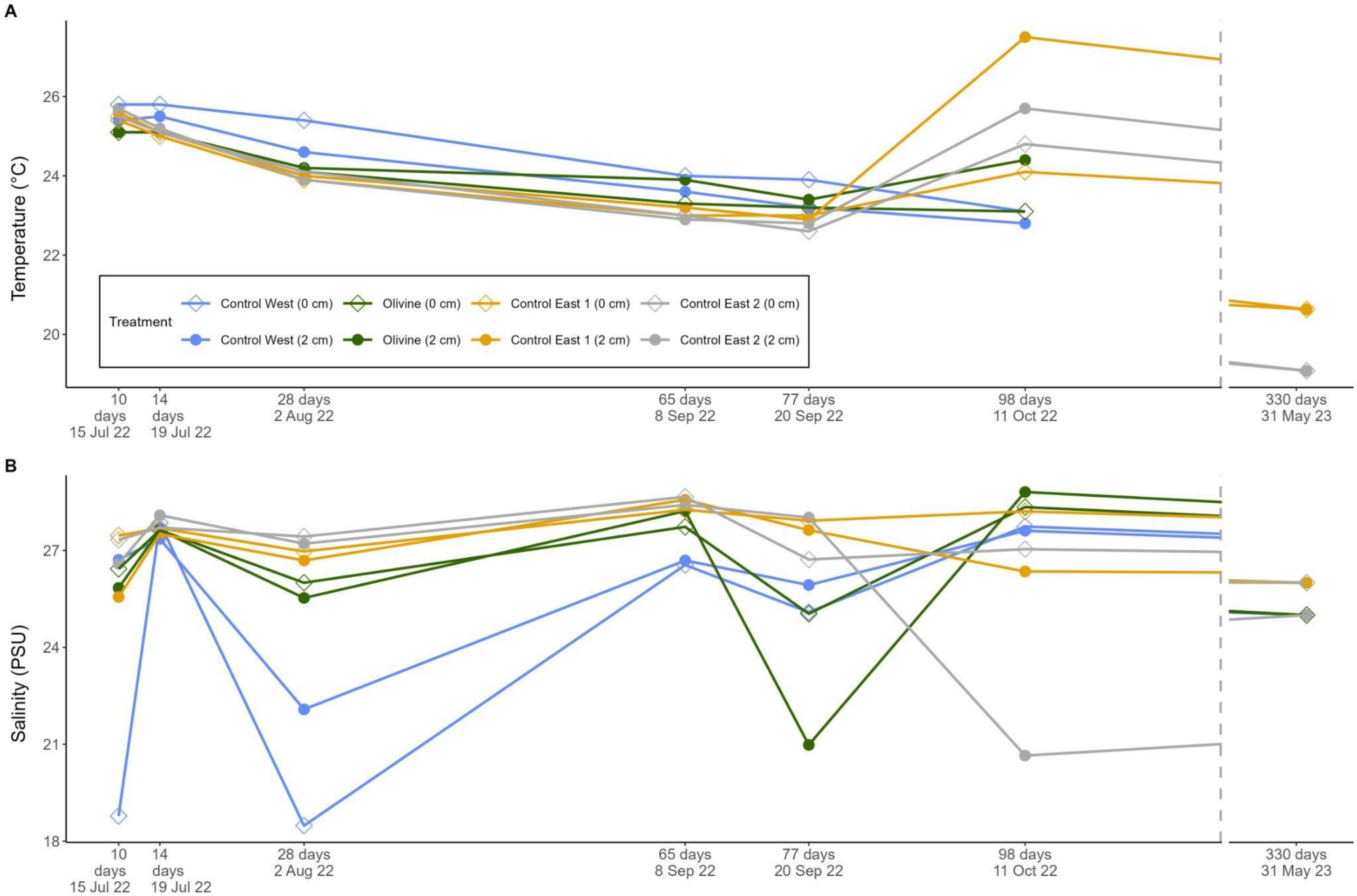

Fig. S3.1 A) Temperature (°C) and B) salinity (PSU) measured during the experiment in bottom water (0 cm) and porewater at 2 cm sediment depth. Colors represent four treatments, shapes represent bottom vs. porewater samples. 'Jul' stands for July, 'Aug' for August, 'Sep' for September, 'Oct' for October, 'Nov' for November. The precision of salinity measurement was approximately 0.07 PSU.

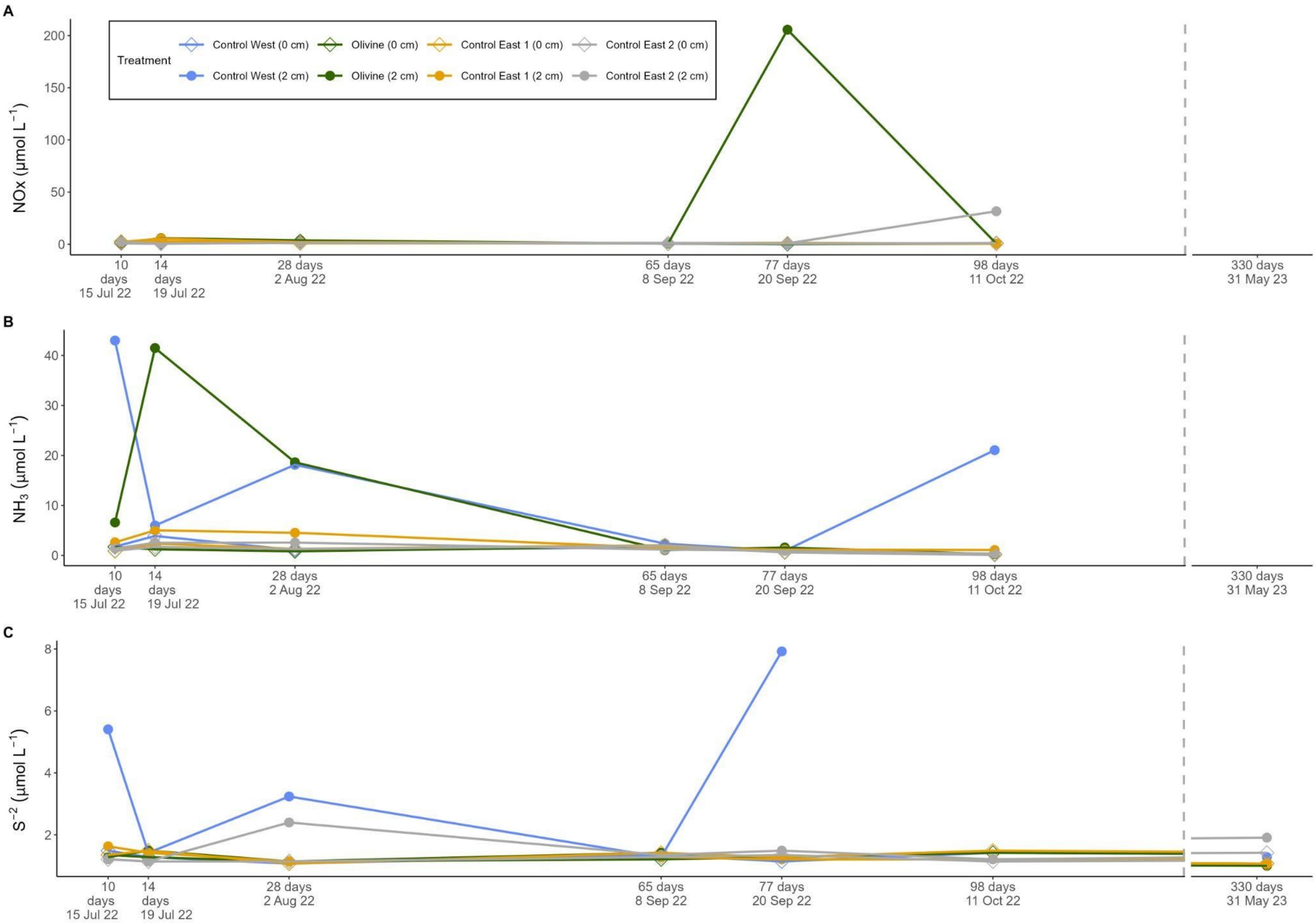

Fig. S3.2 A) Nitrate+nitrite - NO_X^- (µmol L^{-1}), B) ammonia - NH_3 (µmol L^{-1}) and C) sulfide - S^{2-} (µmol L^{-1}) measured during the experiment in bottom water (0 cm) and porewater at 2 cm sediment depth. Colors represent four treatments, shapes represent bottom vs. porewater samples. 'Jul' stands for July, 'Aug' for August, 'Sep' for September, 'Oct' for October, 'Nov' for November. The precision of NO_X^- was approximately 0.14 μmol L^{-1}, NH_3 was approximately 0.16 μmol L^{-1} while of S^{-2} 2.2 μmol L^{-1}.

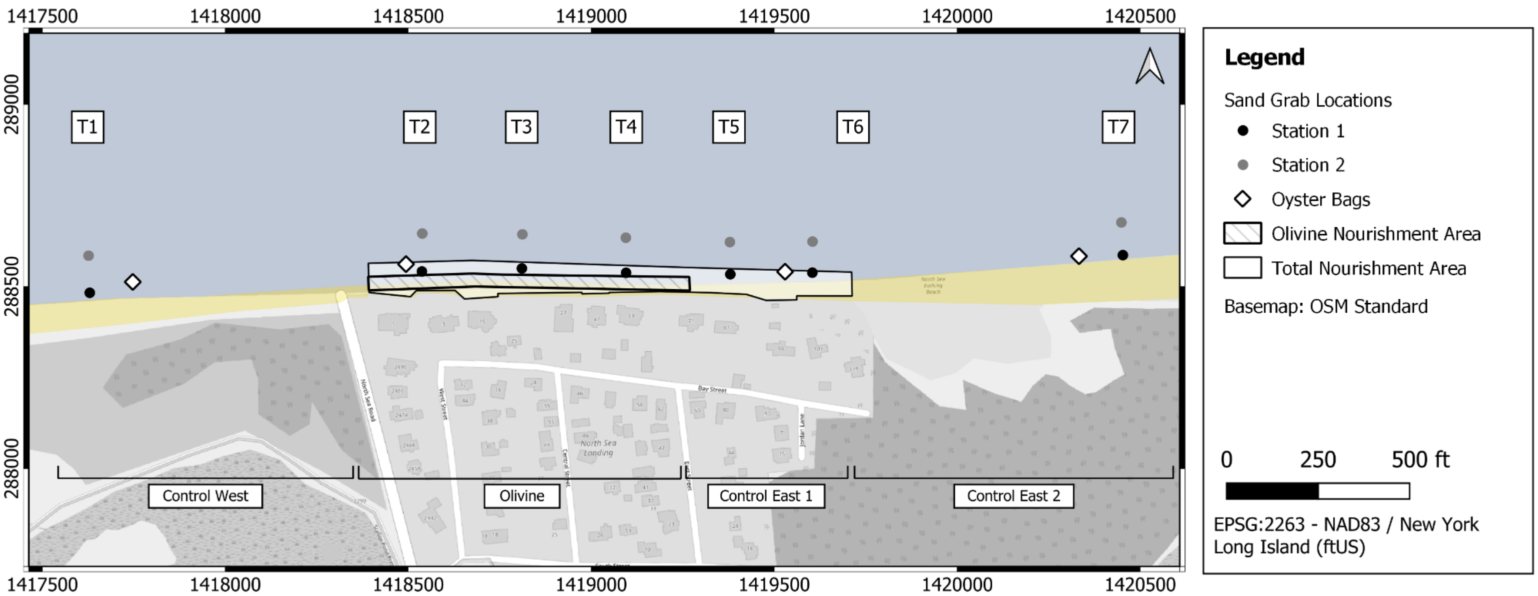

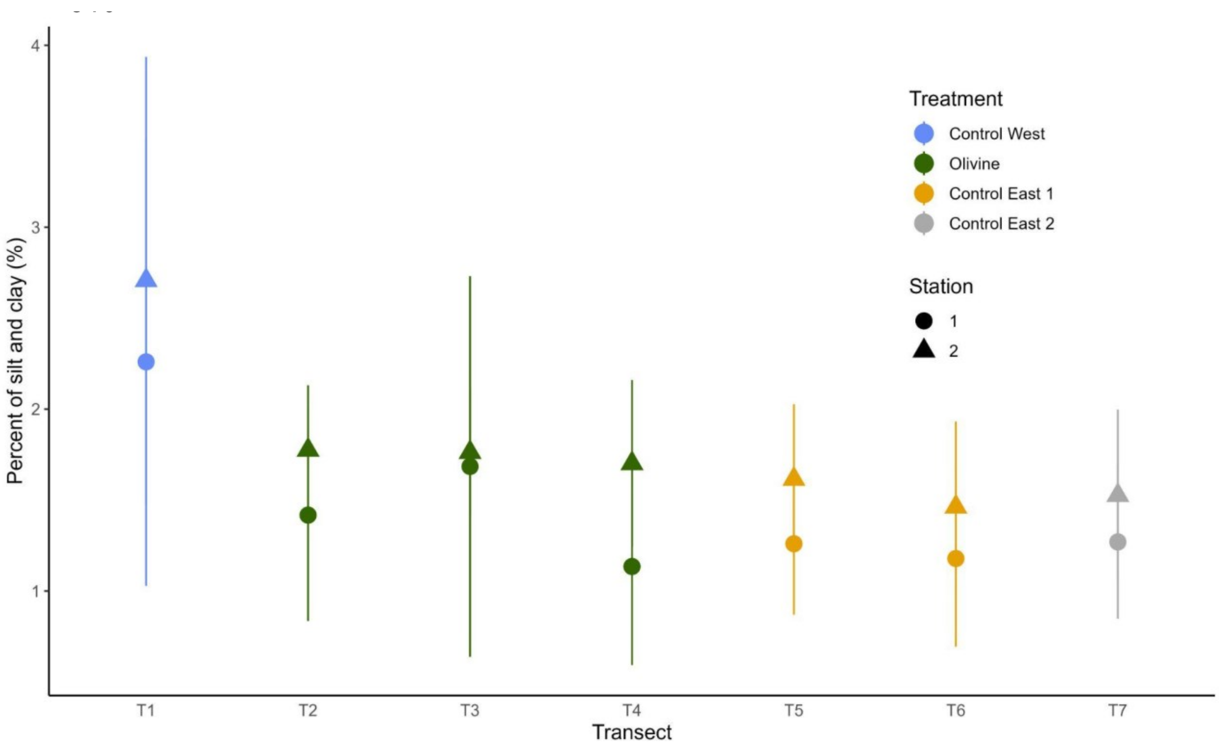

Fig. S3.3 Mean percent silt and clay content calculated from sediment samples collected from seven transects throughout the project area, and two stations per transect, over the course of the experiment (mean ± SD of samples from May, June, August, September, and October 2022, as well as June, August, and October 2023).

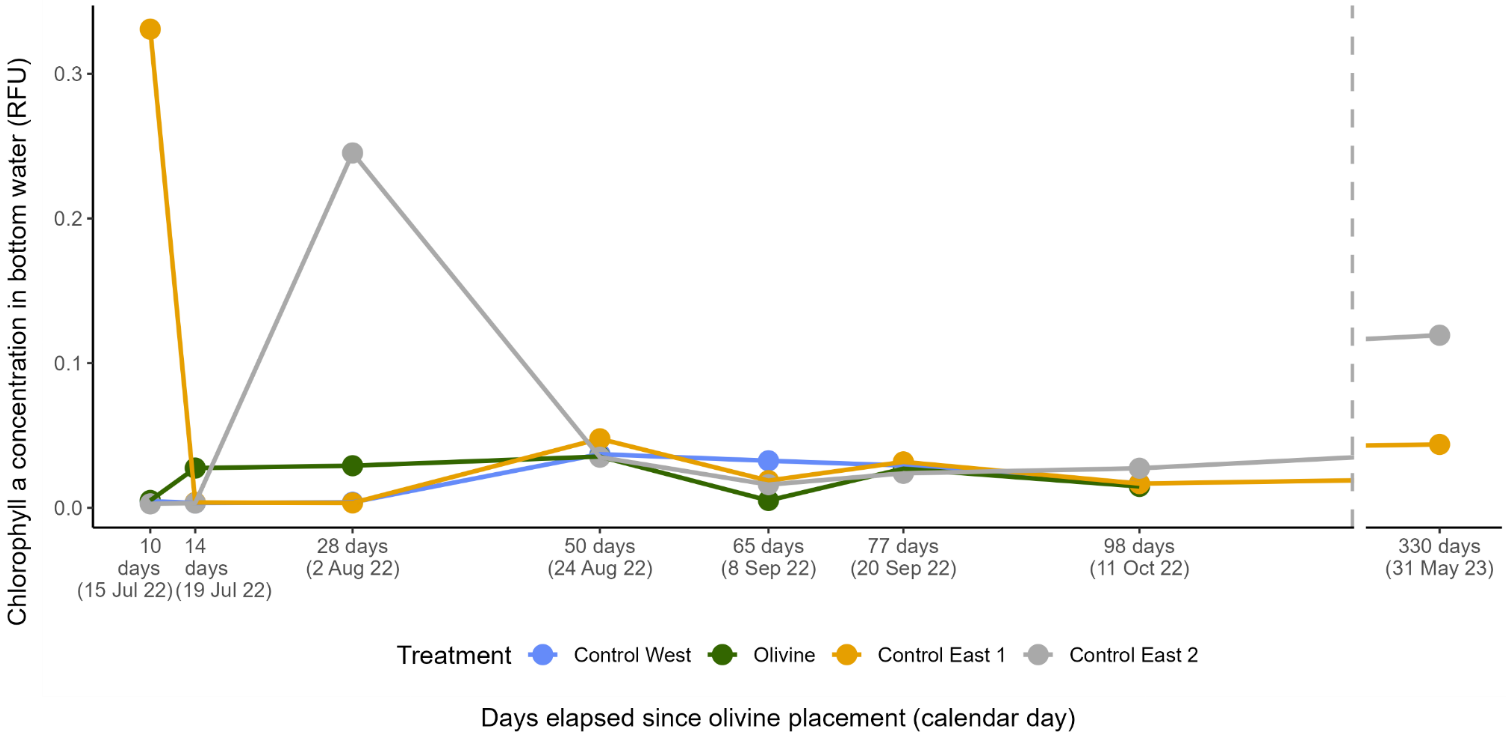

Fig. S3.4 Chlorophyll a concentrations (RFU) measured using an AquaTROLL 500 right above the seafloor throughout the experiment. The instrument measurement error was 0.94 RFU.

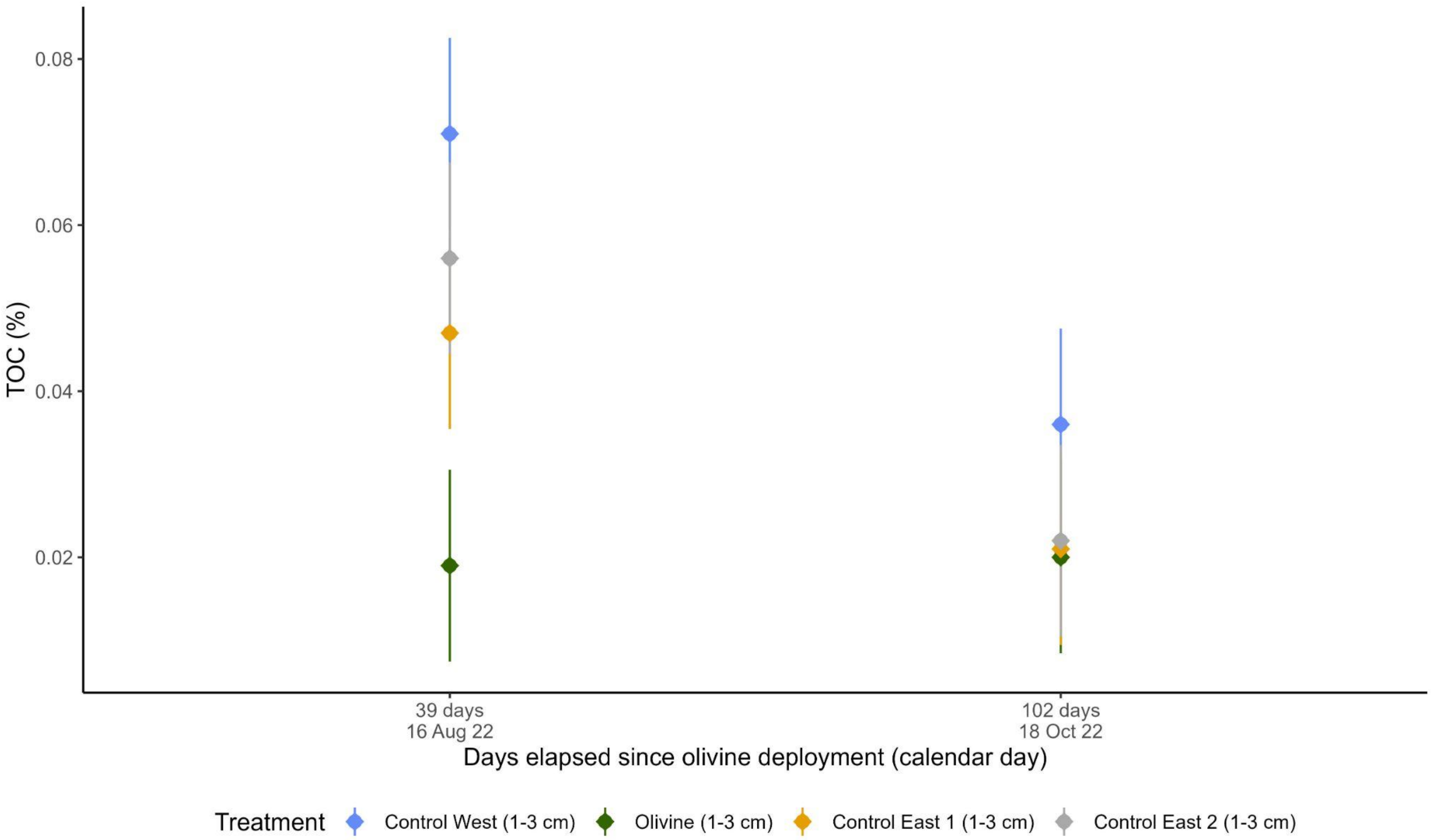

Fig. S3.5 Total organic carbon (TOC %) measured in the top sediment layers (1-3 cm) 39 and 102 days after olivine placement at four treatments. The bars represent measurement error.

Tables

Table S1 Bioconcentration factor measured in oyster tissue at four treatments and three sampling dates. Mean ± SD measured from 12 data points presented.

		BCF Ni		BCF Cr		BCF Co		BCF Fe		BCF Cd	
		mean	stdev	mean	stdev	mean	stdev	mean	stdev	mean	stdev
7 September 2022	Control West	5625	1934	10455	3127	3653	793	5376	1462	44073	5404
64 days elapsed since	Olivine	131	91	2187	671	545	198	2816	854	37323	14553
olivine deployment	Control East 1	1504	477	3721	2556	2156	647	3330	1976	54614	11296
	Control East 2	3583	5233	3582	1882	2543	611	3671	1502	41420	13544
29 November 2022	Control West	1219	447	1293	620	867	173	1933	1002	41405	14977
147 days elapsed since	Olivine	137	990	811	2829	780	1209	1432	2052	49543	14807
olivine deployment	Control East 1	1016	337	1135	7367	2513	436	1381	336	39650	14805
	Control East 2	2960	599	1014	929	1871	813	1336	202	53193	15114
5 May 2023	Control West	1735	393	1815	468	806	158	2115	447	52248	10498
300 days elapsed since	Olivine	178	43	1800	521	822	125	15272	2471	57585	15928
olivine deployment	Control East 1	1358	378	1688	741	2611	579	14402	5086	45051	9702
	Control East 2	4207	1594	1906	294	2382	458	4123	1730	50989	13134

		BCF Pb		BCF Al		BCF Mn		BCF Cu		BCF Zn	
		mean	stdev	mean	stdev	mean	stdev	mean	stdev	mean	stdev
7 September 2022	Control West	2941	850	88680	29592	172	41	254833	81934	404953	189116
64 days elapsed since	Olivine	2021	406	42165	19408	110	25	205976	63722	304358	86589
olivine deployment	Control East 1	2370	941	60448	46683	119	68	288400	132471	374275	145560
	Control East 2	2963	850	78109	42456	175	51	275339	104444	354324	102854
29 November 2022	Control West	5738	1000	1278	5681	74	22	239728	46995	610930	152737
147 days elapsed since	Olivine	5288	946	801	48114	80	78	208913	113526	504400	108960
olivine deployment	Control East 1	4898	1227	650	993	68	21	226026	52632	459257	124048
	Control East 2	5123	785	556	243	79	18	253844	51557	555280	114343
5 May 2023	Control West	2608	345	7168	11778	86	44	238984	42497	311658	62785
300 days elapsed since	Olivine	4880	841	2889	2024	94	74	216720	23804	502833	53293
olivine deployment	Control East 1	7605	1781	2185	2649	749	312	202057	60165	448766	106476
	Control East 2	9965	1558	2852	1587	315	114	282642	100381	316862	94345

Table S2 Comparison of mean Ni, Cr and Co body burden in oysters and other bivalves measured in the current study and other studies worldwide presented in Fig. 5 in the main text.

861

Study	**Species**	**Ni [µg g dw^{-1}]**	**Cr [µg g dw^{-1}]**	**Co [µg g dw^{-1}]**	**Reference**
OYSTERS					
US, Olivine treatment, Control West treatment (this study)	***C. virginica***	**1.69 – 3.35** **1.64 – 5.23**	**0.13 – 0.33** **0.16 – 0.59**	**0.22 – 0.32** **0.24 – 0.45**	**This study**
US East Coast	*C. virginica,*	0.9 - 4.2	-	-	Goldberg et al. 1982 (US Mussel Watch)
US Gulf Coast	*C. virginica, O. equestris*	0.5 - 7.3	-	-	Goldberg et al. 1982 (US Mussel Watch)
San Diego Bay, US	*C. gigas*	0.10 to 0. 13	0.13 to 0.27	-	Talley et al. 2022
Gulf of California, Mexico	*C. gigas*	9.41 ± 11.33	22.29 ± 30.23		Jonathan et al. 2017
France	Different species	0.34 ± 0.07	0.07 ± 0.00	0.05 ± 0.00	Lehel et al. 2023
Queshm Islands, Iran	*Saccostrea cucullata* (Born, 1778)	2.47 – 4.51	-	-	Fatemi et al. 2011
Pulicat coastal lake, India	*Crassostrea madrasensis* (Preston, 1996)	5.2 – 6.2	2.5 – 2.8	-	Priya et al. 2010
Gulf of Chabahar, Oman	*S. cucullata*	15. 4 – 38.0	12.7 – 27.9	-	Bazzi, 2014
Milliardaires Bay, Cote d'Ivoire	*Crassostrea gasar* (Dautzenberg, 1891)	35.97 - 179.45	-	-	Tuo et al. 2019

Mandinga Lagoon, Maxico	*C. virginica*	-	6.43 ± 8.04	-	Guzman-Garcia 2009
China	Different species	0.33-31.5	0.28-11.0	-	Lu et al. 2019
MUSSELS OR CLAMS					
Norway – Kirkebukten 4 years of natural olivine exposure	Different species	1.1 – 3.5	0.9 – 4.1	-	Gjesdal and Solheimslid, 2016
Norway – Kirkebukten 12 weeks of controlled olivine exposure	*Mytilus edulis* (Linnaeus, 1758)	0.5 – 1.0	0.5 – 0.9	-	Bojum and Gjesdal, 2020
San Diego Bay, US	Different species	0.31 – 0.61	1.33 – 1.85	-	Talley et al. 2022
Bull Island, Dublin Bay	*Cerastoderma edule* (Linnaeus, 1758)	17.8 - 53.82	-	-	Wilson 1983
Italy	Different species	0.76 ± 0.97	0.24 ± 0.16	0.11 ± 0.14	Lehel et al. 2023
Southern Spain	*Chamelea gallina* (Linnaeus, 1758)	0.39 – 0.64	0.13 - 0.89	-	Usero et al. 1996